Development of a new EGFR receptor PET imaging agent based on the 3-cyanoquinoline core: synthesis and biological evaluation

Federica Pisaneschi,[a,c] Elham Shamsaei,[a] Quang-de Nguyen,[a] Matthias Glaser,[b] Edward Robins,[b] Maciej Kaliszczak,[a] Graham Smith,[a] Alan C. Spivey,[c] Eric O. Aboagye[a*]*

a) Comprehensive Cancer Imaging Centre, Imperial College London, Faculty of Medicine, Hammersmith Hospital Campus, Du Cane Road, London, W12 0NN, United Kingdom;

b) Medical Diagnostic Discovery (part of GE Healthcare) at Hammersmith Imanet Ltd, Hammersmith Hospital, Du Cane Road, London W12 0NN, United Kingdom;

c) Department of Chemistry, Imperial College London, South Kensington Campus, SW7 2AZ, United Kingdom.

RECEIVED DATE (to be automatically inserted after your manuscript is accepted if required according to the journal that you are submitting your paper to)

CORRESPONDING AUTHOR FOOTNOTE

To whom correspondence should be addressed. Phone: + 44 (0)20-8383-3759, Fax: + 44 (0)20-8383-2029, E-mail: eric.aboagye@imperial.ac.uk; Phone +44(0)20-8383-3720, Fax +44 (0)20-8383-1783, E-mail: f.pisaneschi@imperial.ac.uk.

Abstract

The Epidermal Growth Factor Receptor (EGFR/c-ErbB1/HER1) is overexpressed in many cancers including breast ovarian, endometrial and non-small cell lung cancer. PET imaging of EGFR receptor status could enable the biology of the receptor in entire heterogeneous primary tumors and/or metastases to be studied in humans. This in turn should lead to more objective ways of assessing prognosis or predicting response to drug therapy. To achieve this goal we designed and synthesized a small library of fluorine containing compounds based on a 3-cyanoquinolines core. A lead compound, **17,** incorporating 2′-fluoroethyl-1,2,3-triazole was selected based on its low affinity (1.81 ± 0.18 nM) for EGFR kinase, good cellular potency, low lipophilicity and good metabolic stability. "Click" labeling afforded the ^{18}F-labeled tracer, [^{18}F]**17,** in 37.0±3.6 % decay corrected radiochemical yield from azide [^{18}F]-**16** and >99% radiochemical purity. The compound showed good stability *in vivo* and a 4-fold higher uptake in A431 tumor xenografts relative to muscle. Furthermore, the radiotracer could be visualized in A431 tumor bearing mice by small animal PET imaging. Tracer [^{18}F]**17** is a candidate radiotracer for further evaluation for imaging of EGFR status.

Introduction

Epidermal growth factor receptor (EGFR/c-ErbB1/HER1) is overexpressed in breast, ovarian and other human cancers.[1, 2] EGFR along with the other three members of the HER family (HER2, HER3 and HER4) is a transmembrane glycoprotein with an extracellular ligand-binding domain, a transmembrane domain, and an intracellular domain with tyrosine kinase activity. EGFR is activated by binding to a variety of ligands including EGF, amphiregulin and TGF-α.[3] Once activated it is believed to undergo homo- or heterodimerisation followed by activation of the intrinsic protein tyrosine kinase, autophosphorylation and activation of intracellular signal transduction pathways such as phosphatidylinositol-3-kinase (PI3K)/AKT and ras/raf/MEK/MAPK.[4-6] Blocking EGFR activity therefore appears to be a potent strategy in the treatment of cancer, and various anti-EGFR therapies have been recently developed. Along with the development of monoclonal antibody inhibitors (*e.g.* Cetuximab), which are currently in use for the treatment of breast cancer,[7, 8] a new arsenal of small molecules designed to inhibit the intracellular tyrosine kinase activity have arisen in recent years. Certain compounds in this class have already been approved for clinical use (Gefitinib/Iressa,[9] Erlotinib/Tarceva[10]) whilst others are under preclinical or clinical investigation [*e.g.* Neratinib, Pelitinib (**1**, Figure 1)].[11, 12] Efficacy of these small molecule inhibitors is largely dependent on competition with the naturally occurring ATP for binding at the enzyme active site. Unfortunately, clinical use of these inhibitors has led to the emergence of drugs resistant tumors *via* gene amplification or mutation in the kinase domain.[13] Additionally, the binding site has a high degree of similarity to many other tyrosine kinases complicating the search for selective inhibitors. Consequently, there remains an urgent need for the development of new, more potent and selective inhibitors.

Molecular imaging techniques, such as PET (Positron Emission Tomography) have the potential to provide insights into EGFR biology. Potentially PET with EGFR probes can non-

invasively determine whether the target protein is overexpressed in a specific primary tumor or metastasis *in vivo*, the magnitude and duration of receptor occupancy, and target-drug interactions (including possibly the functional consequence of mutations that lead to reduced EGFR-drug interactions). As reviewed by Mishani *et al*,[14] a number of the previously reported therapeutics have been labeled with radionuclides, including radiometals and radiohalogens, as potential ligands for imaging EGFR. Among the monoclonal antibodies, ^{64}Cu-DOTA-cetuximab showed high uptake in A431 tumors although a significant uptake in the liver was observed, partly due to the dissociation of the ^{64}Cu from the DOTA chelator.[15, 16] Attempts to develop small molecule imaging agents have mainly focused on the replacement of radiohalogens in the original positions of those compounds developed for therapy. All these compounds are *reversible* inhibitors of EGFR based on a 4-anilinoquinazoline core.[17-19] Although they have shown promise *in vitro*, they have not demonstrated adequate signal to noise ratio for PET radioimaging of EGFR-overexpressing tumors in animal models. This failure can be attributed in part to their relatively high lipophilicity (i.e. Log*P*) as well as competition of the ligands with intracellular ATP leading to their rapid washout from cells. In light of these limitations, a new generation of imaging agents was designed, based on *irreversible* EGFR inhibitors. This new class of molecules usually bears an electrophile on the C-6 position of the quinazoline core which binds covalently *via* a Cys 773 present in the tyrosine kinase binding site of EGFR. The covalent bond overcomes the washout caused by the abundance of intracellular ATP and usually results in an increase of potency (Yun *et al.* estimated that the potency of a covalent inhibitor is equivalent to a 0.2 nM inhibitor).[20] During the last few years, Mishani *et al*. reported ^{11}C, ^{18}F and ^{124}I anilinoquinazoline radiolabeled irreversible inhibitors based on this concept and recently Neumaier *et al.* has also disclosed an ^{18}F labeled potential probe (Figure 1).

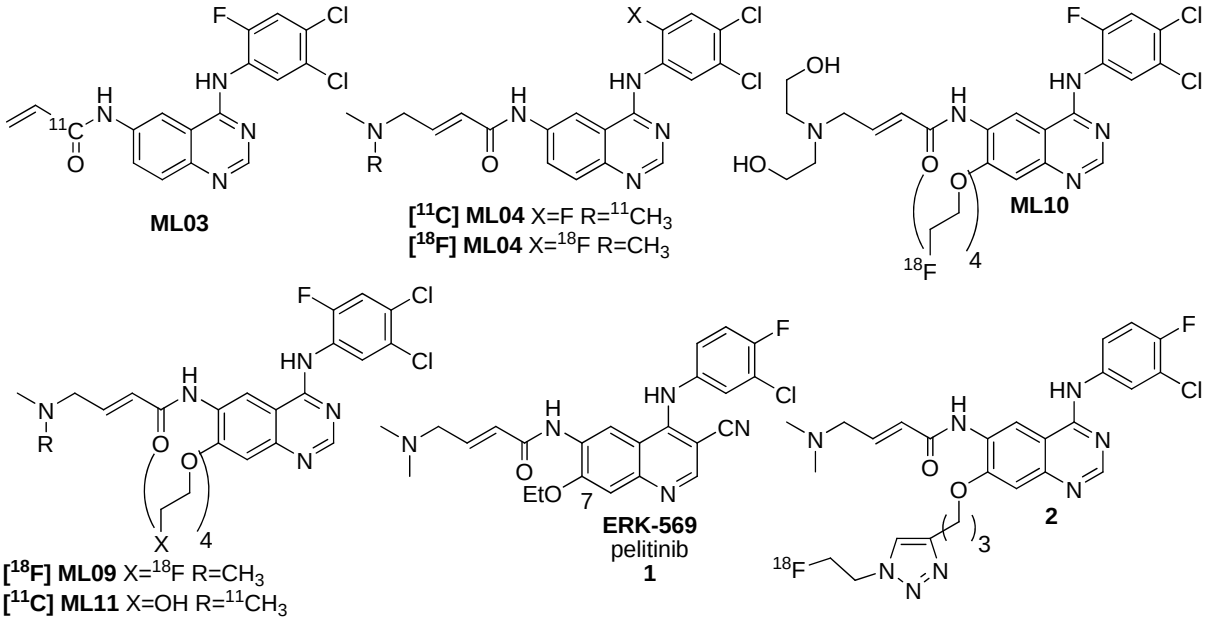

Figure 1. Chemical structures of EGFR therapeutics and imaging agents. While the acrylamide [^{11}C]-ML03[21] showed a remarkable inhibitory effect *in vitro* (cell free assays and A431 cells), it was not suitable as a PET imaging probe due to fast metabolic degradation and low tumor uptake. Radioimaging agents [^{11}C]- and [^{18}F]-ML04[22, 23] performed better *in vivo* in biodistribution studies but resulted in non-specific uptake probably due to their high Log*P*. In order to lower Log*P* but maintain their ability to penetrate the cell, [^{18}F]-ML09/ML10 and [^{11}C]-ML11 were synthesized and are currently under investigation.[24, 25] In late 2009 anilinoquinazoline **2** labeled by a click chemistry strategy was reported by Neumaier *et al.*[26] EGFR overexpressing PC9 tumor xenografts could be visualized by PET following injection of **2** into mice.

The aim of the work described here was the synthesis and biological evaluation of ^{18}F radiolabeled irreversible imaging agents based on the 3-cyanoquinoline core, first reported by Wissner *et al* in 2000.[27, 28] The fluorine-18 moiety was planned to be introduced at the end stage of the synthesis by means of an easy and efficient methodology. This constitutes an incontrovertible advantage for obtaining high radiochemical yields. In addition the long half life time of fluorine permits the use of those probes at sites that lack an on-site cyclotron.

Molecular modeling studies indicate that the 3-cyano group in lead compound **1** (Figure 1) replaces the nitrogen of the quinazoline core and hydrogen bonds to Thr 830.[28] In quinazolines this interaction is achieved from N-3 *via* a molecule of water; because the 3-

cyano interaction with Thr 830 is expected to be more entropically favored than that through a binding complex with water, it was expected that 3-cyano quinolines would likely provide more specific imaging signals than quinazoline analogues. For cyanoquinolines, the aniline moiety at C-4 lies in the hydrophilic pocket of the enzyme. As in the Mishani quinazoline series, a C-6-Michael acceptor was envisaged to covalently bind to Cys 773 of the EGFR binding site with the proximal tertiary amine acting as an internal base. The C-7-ethoxy group points to the outside of the binding site and does not appear to play an important role in binding.

Taking these observations into consideration it was decided that the lead compound **1** would be modified by the addition of a fluorine containing group at a position anticipated to be non-essential for binding. Initially, different fluorine containing groups were introduced at the nitrogen of the Michael acceptor at C-6. We then replaced the nitrogen of the Michael acceptor with a triazole derivative. As labels at the C-7 position were found to be preferable than those at the C-6 position,[29] we also replaced the 7-ethoxy group with a fluoroethoxy group. The Michael acceptor was modified with a secondary amine because the latter has been reported to present a higher metabolic stability than a tertiary amine.[30]

Results

Chemistry

The quinoline advanced intermediate **6** together with the Michael acceptors **3**, **4**[28, 31] and **5**[32] and quinoline based EGFR inhibitor "standard" **1**[28, 31] were synthesized accordingly to the literature procedures (Figure 2).

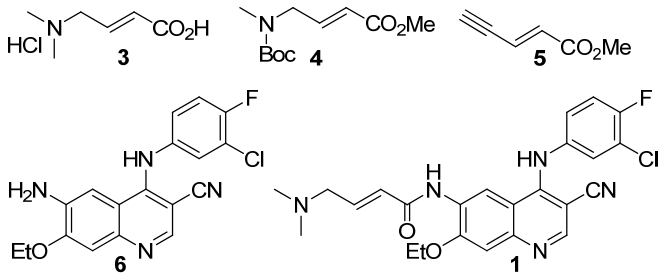

Figure 2. Literature compounds prepared for this work.

Michael acceptor **8** was obtained by reacting commercially available methyl 4-bromocrotonate (**7**) with propargyl amine at –20 °C then protecting *in situ* the resulting secondary amine as a Boc carbamate (Scheme 1).

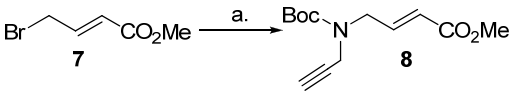

Scheme 1. *Reagents and Conditions*: a. propargyl amine, Et_3N, THF, –20 °C, 4 h then Boc_2O, –65 °C→ rt, (49%).

The coupling at C-6 of quinoline **6** and methyl esters **4**, **5** and **8** was performed by $AlMe_3$ mediated amidation using dry CH_2Cl_2 to give amides **9**, **11** and **12** in yields of 47%, 68% and 20%, respectively. The Boc group in compound **10** was removed with 10% conc. HCl in

dioxane and the product precipitated as the hydrochloride salt. This salt was neutralized by treating with K_2CO_3 in H_2O overnight, during which time the free amine **10** precipitated from the solution in 78% yield (Scheme 2). Quinoline **10** was obtained spectroscopically pure and used in the following step with the need of further purifications.

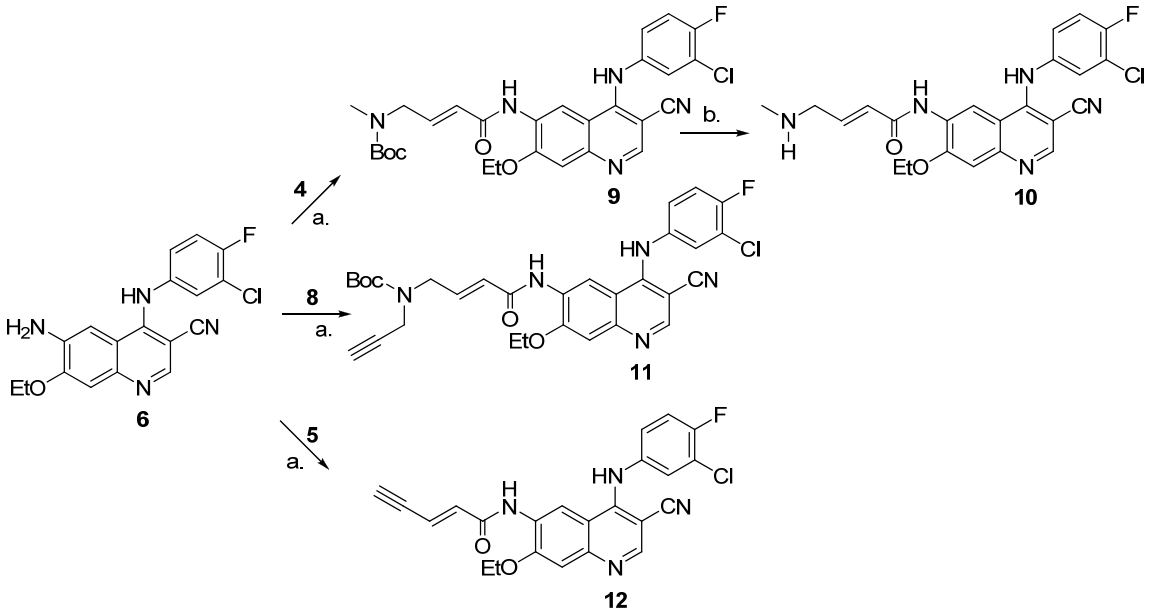

Scheme 2. *Reagents and Conditions*: a. $AlMe_3$, CH_2Cl_2, rt, (**9**: 47 %, **11**: 68%, **12**: 20%). b. *i.* dioxane:HCl, 10:1, rt, 30 min. *ii.* K_2CO_3, H_2O 14 h (78 %).

Derivatisation of *N*-methyl amine **10** in a manner amenable to introduction of ^{18}F radiolabel was achieved by two methods: alkylation and reductive amination. Alkylation of amine **10** with 1-fluoro-2-mesyloxy ethane (**15**) in CH_2Cl_2 gave the *N*-fluoroethyl product **13** in 33% yield along with unidentified by-products which made the final purification difficult and limited the yield. As the *N*-alkylation reaction could not be developed into an efficient method to introduce the desired fluorine-contained substituent, reductive amination was explored as an alternative method. Consequently, quinoline **10** was transformed into 4-fluorobenzyl product **14** by treatment with 4-fluoro benzaldehyde and $NaBH(OAc)_3$. Compound **14** was obtained in a 21% unoptimized yield (Scheme 3).

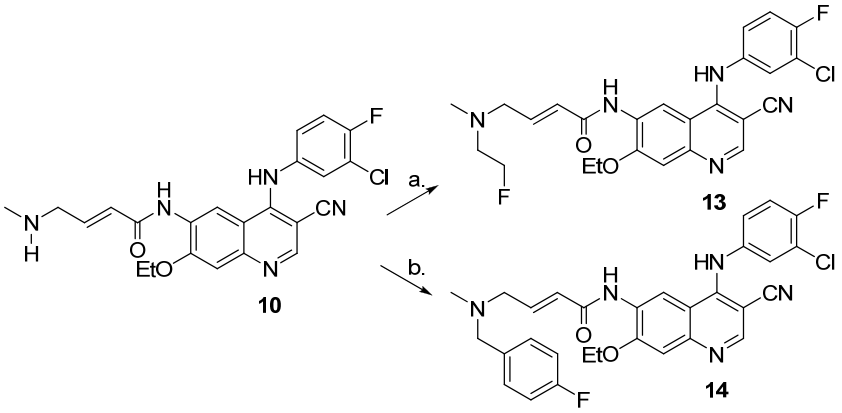

Scheme 3. *Reagents and Conditions*: a. **15**, Et_3N, CH_2Cl_2, 18 h at rt and 24 h at reflux (33%). b. *p*-fluoro-benzyaldehyde, AcOH, $NaBH(OAc)_3$, 1,2-dichloroethane, 14 h (21%)

Derivatisation of *N*-Boc-propargylamine **11** in a manner suitable for ^{18}F radiolabel introduction was envisaged to be achieved by copper(I) catalyzed Huisgen 1,3-dipolar cycloaddition with a fluorine containing azide partner.[33, 34] The "click" reaction between azides and terminal acetylenes to afford 1,2,3-triazoles has been widely used in the last decade as a tool for the coupling of two building blocks in many fields of chemistry.[35] As these reactions are in principle selective, fast and high yielding; this approach appeared attractive for the incorporation of the ^{18}F radionuclide into this class of inhibitors. Quinoline precursor **11** was then reacted with 1-fluoro-2-ethyl azide (**16**)[33] under Cu(I) catalysis and microwave irradiation[36] to give the Boc protected analogue of quinoline **17** which was treated with HCl in 1,4-dioxane to form the final quinoline **17** as an HCl salt. (Scheme 4).

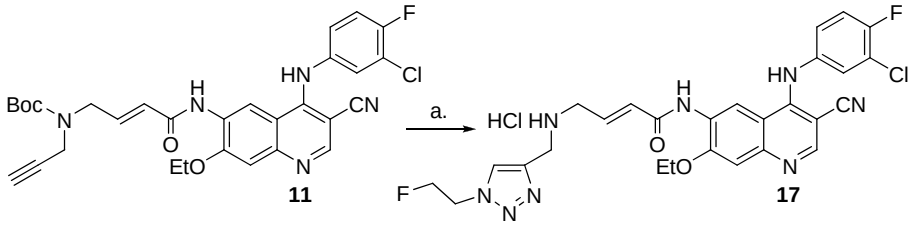

Scheme 4. *Reagents and Conditions*: a. *i.* **16**, Cu powder, $CuSO_4$, water, MW 125 °C, 15 min (19%); *ii.* Dioxane : HCl, 10:1, 1 h (99%).

Analogously, derivatisation of the eneyne containing quinoline **12** was effected by "click" cycloaddition with azide **16**. This reaction gave quinoline **18** directly without the requirement for any further synthetic manipulations (Scheme 5)

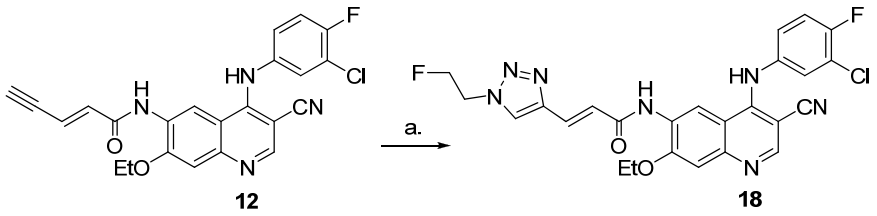

Scheme 5. *Reagents and Conditions*: a. **16**, Cu powder, $CuSO_4$, water, MW 125 °C, 15 min (32%).

Quinoline **24** was designed as a direct analogue of quinoline **10** but containing a 2-fluoroethoxy group in place of the C-7 ethoxy group. Since the C-7 is also potentially susceptible to metabolism (*O*-dealkylation), this substitution might increase metabolic stability. The synthesis of quinoline **24** started from quinoline **19**, obtained as HCl salt from the literature procedure, which was initially treated with the anion exchange resin AmberSep 900 OH to remove any traces of HCl. The ethoxy group was then removed by treating with BBr_3 in CH_2Cl_2 to give 7-hydroxyquinoline **20**. This quinoline was treated with 1-fluoro-2-mesyloxy ethane (**15**) and K_2CO_3 in DMF to give 7-(2-fluoroethoxy)quinoline **21** in 75% yield from **19** and the acyl group was removed by heating in conc. HCl and water. The resulting 6-aminoquinoline **22** was linked to the Michael acceptor ester **4** using $AlMe_3$ mediated amidation in toluene. The Boc group was removed by treatment with HCl in 1,4-dioxane yielding quinoline **24** as the HCl salt in 67% yield (Scheme 6).

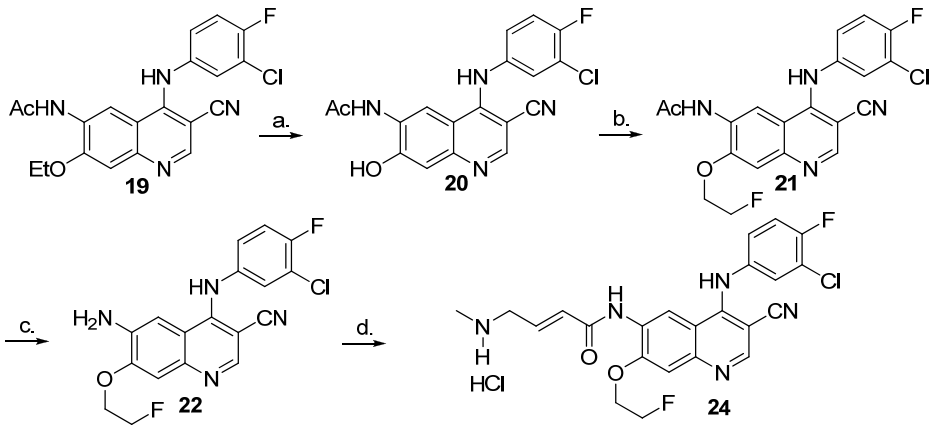

Scheme 6. *Reagents and Conditions*: a. BBr_3, CH_2Cl_2, rt (40%); b. **15**, K_2CO_3, DMF, 70 °C, 18 h (83%); c. conc. HCl, H_2O, 120 °C, 1.5 h (53%); d. *i.* **4**, $AlMe_3$, toluene, rt, 14 h (61%), *ii.* conc. HCl, dioxane, rt (67%).

Radiochemistry

Alkyne containing quinoline **25** was obtained from compound **11** by treatment with conc. HCl in 1,4-dioxane in quantitative yield. Compound **25** was labeled by cycloaddition under Cu(I) catalysis by using [^{18}F]-fluoroethyl azide [^{18}F]-**16** following a published procedure (Scheme 7).[37-39]

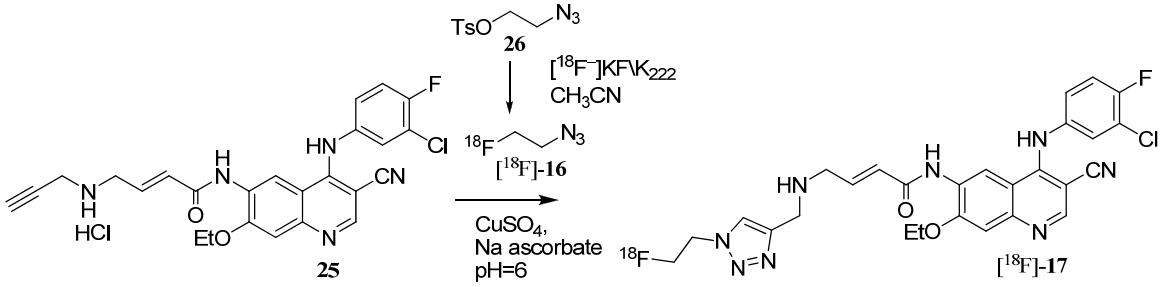

Scheme 7. Radiosynthesis of quinoline [^{18}F]-**17**

[^{18}F]-Fluoro ethyl azide [^{18}F]-**16** was synthesized from the corresponding tosyloxy ethyl azide **26** and [^{18}F]KF/Kryptofix 222 at 80 °C for 15 min. The product was purified and collected by distillation; it was obtained with a 42.2±4.2 % (n=12) decay corrected radiochemical yield. Precursor **25** was dissolved in MeCN/water, 1:1, mixed to the catalytic system and then

heated with the azide [^{18}F]-**16** in MeCN at 80 °C for 15 min. The crude compound [^{18}F]-**17** was purified by semipreparative HPLC in a 37.0±3.6 % (n=12) decay corrected radiochemical yield from azide [^{18}F]-**16** and >99% radiochemical purity. Compound [^{18}F]-**17** was formulated by solid-phase extraction with an efficiency of ~90%. The identity of [^{18}F]-**17** was confirmed by co-elution with the non-radioactive compound and obtained with a specific activity up to 685 GBq/μmol. The radioimaging agent [^{18}F]-**17** was stable for >4 h after formulation in phosphate buffered saline (PBS). The radiosynthesis including formulation took 3 h in total.

EGFR kinase activity.

A key design goal is the introduction of radiolabeled motifs without, at the very least, detriment to EGFR affinity relative to the starting quinoline **1**. Therefore, assessment of the EGFR tyrosine kinase activity of control quinolines **1** together with quinolines **10**, **13**, **14**, **17**, **18**, **24** and **25** was carried out using a cell free kinase activity inhibition assay as detailed in the Experimental section. BPDQ,[40] a quinazoline based EGFR inhibitor was also included in this assay as a further reference standard. Concentrations of the compounds that inhibited EGFR kinase activity by 50% (IC_{50}) were calculated and are reported in Table 1.

Table 1. EGFR kinase activity inhibition profile for quinolines **1**, **10**, **13**, **14**, **17**, **18**, **24** and **25**.

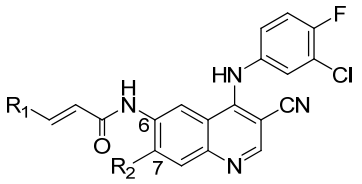

			IC50 (nM)		
	R_1	R_2	EGFR kinase activity	A431 EGFR autophosphorylation[a]	Log*P*[b]
BPDQ			0.81 ± 0.01	>1000	2.57
1	CH_2NMe_2	OEt	0.24 ± 0.02	8.02 ± 0.75	4.18
10	CH_2NHMe	OEt	0.25 ± 0.06	5.35 ± 1.52	3.80
13	$CH_2N(Me)CH_2CH_2F$	OEt	0.80 ± 0.04	23.02 ± 12.0	4.38
14	$CH_2N(Me)$-4-fluoro benzyl	OEt	0.57 ± 0.12	16.52 ± 8.38	6.05
17	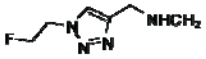	OEt	1.81 ± 0.18	21.97 ± 9.06	3.85
18		OEt	4.05 ± 0.57	>1000	4.45
24	CH_2NHMe	OCH_2CH_2F	0.29 ± 0.03	8.12 ± 2.03	3.64
25	$CH{\equiv}CCH_2NHMe$	OEt	0.03 ± 0.01	60.2 ± 17.1	3.94

[a]data were extracted from the concentration *vs* p-EGFR/total EGFR western blot absorbance ratio. Data are mean±sem, n= 3 replicates.

[b]LogP are calculated by ChemAxon's MarvinSketch, version 5.2.6.

All eight compounds inhibited EGFR kinase activity with IC_{50} values in the low- or sub-nanomolar range which compares well with that of BPDQ (Table 1). Compound **1** appeared more potent than previously reported by Wissner *et al.*[28] presumably because of differences in the assay used. The same authors have shown that **1** functions as an irreversible inhibitor of EGFR. The IC_{50} values are probably best interpreted in the context of reversible inhibition, as well as irreversible covalent binding resulting from interactions with the Michael acceptor (and other reactive) moieties. The sub-nanomolar kinase activity observed with compounds **1** and **10** was retained in compounds **13** and **14** demonstrating tolerance for small and large fluorine-containing substituents on the tertiary amine group. Fluorine substitution at the C-7

position was also tolerated as reflected in the comparably low IC_{50} measured for compounds **10** and **24**. Of interest to application of 'click' radiochemistry, substitution of fluoroethyl triazole on the Michael acceptor – exemplified by quinolines **17** and **18** – was tolerated, with quinoline **17** being two-fold more active than **18**. The activity of triazole derivatives **17** and **18** was reduced 10-20 fold relative to quinoline **1**; the reason for this is unclear since previous modeling studies place the amine substituents at the edge of the kinase pocket. In addition, bulk substitution was accepted in the case of quinoline **14**. Surprisingly the activity of the alkyne-containing quinoline **25** was in the picomolar range (30 pM) probably due to a previously undocumented π–π interaction that may also help to explain the high affinity of fluorobenzyl quinoline **14**.

Cellular activity and lipophilicity.

Given the encouraging inhibitory EGFR kinase activity of the compound series in the cell-free system, we examined cellular activity - the ability of the compounds to be transported across cell membranes and to inhibit EGFR autophosphorylation - in highly EGFR-expressing A431 cells.[41] Following the reversible binding protocol previously reported by Rabindran *et al*.,[11] we measured the potency of the compounds to inhibit autophosphorylation of EGFR after 3 h of drug incubation (and a further 2 h of washing with drug free medium). Typical immunoblots demonstrating inhibition of EGFR autophosphorylation are shown in Figure 3. In these studies the drug did not inhibit the expression of total EGFR protein. The inhibitory activity of compounds **1**, **10**, **13**, **14**, **17**, and **24** on cellular EGFR autophosphorylation, (Table 1) translated well from that assessed in the cell-free system, with IC_{50} values in the low nanomolar range. Interestingly, no cellular activity was apparent when dosing with quinoline **18**. Furthermore, the cellular activity of quinoline **25** was in the low nanomolar range

indicating that, although potent, the high affinity of this alkyne in the kinase assay did not directly translate into cellular activity.

The calculated Log*P* of the series ranged between 3.64 and 6.05 with fluorobenzyl substitution giving the highest Log*P* value. Log*P* provides an estimate of the compound's ability to pass through a cell membrane. Compounds with a Log*P* > 5 are known to be nondruggable as defined by Lipinski's rule of 5.[42] The Log*P* of **14** being above the threshold may be sufficient to discard this compound at this stage. All the other compounds have a Log*P* > 3 which suggests that no major difference could be drawn in terms of permeability among the different member of the library.

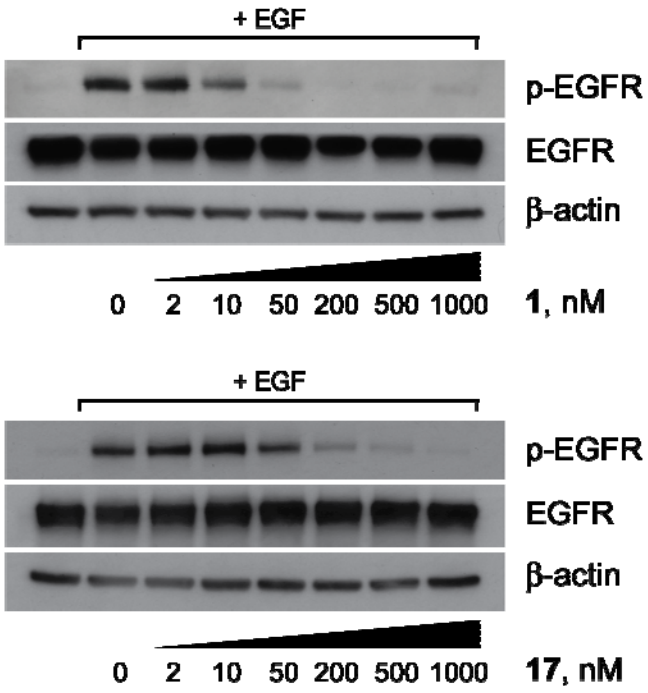

Figure 3. Cellular activity of quinolines **1** and **17** assessed by Western blots analysis of phosphorylated EGFR (p-EGFR) and total EGFR (EGFR).

Cellular uptake of radiotracer [^{18}F]17

Preliminary assessment of the suitability of [^{18}F]**17** as a candidate PET radioligand was carried out by incubation in A431 cells. It has been reported that the uptake of structurally related anilinoquinazolines are modulated by the multi-drug resistant phenotype,[43] potentially confounding the EGFR-specific effects. Thus, we studied the uptake of compound [^{18}F]**17** in the presence of verapamil, an inhibitor of the multi-drug resistant transporters. Uptake of [^{18}F]**17** was also modulated by pre-incubation with A431 cells of the natural ligand EGF and a 200 nM solution of quinoline **10** as a blocking agent. From Figure 4 it is evident that addition of EGF increased the cellular uptake of compound [^{18}F]**17** by 22% and the pre-treatment with compound **10** decreased cellular uptake by 30%. In a separate study, also shown in Figure 4, comparative uptake of [^{18}F]**17** was carried out in A431 and in the low EGFR expressing MCF-7 breast carcinoma cell line. Uptake of [^{18}F]**17** was two fold higher in the EGFR overexpressing A431 cell line relative to MCF-7 cells. Experiments reported in Figure 4 demonstrated an EGFR dependant uptake of [^{18}F]**17**.

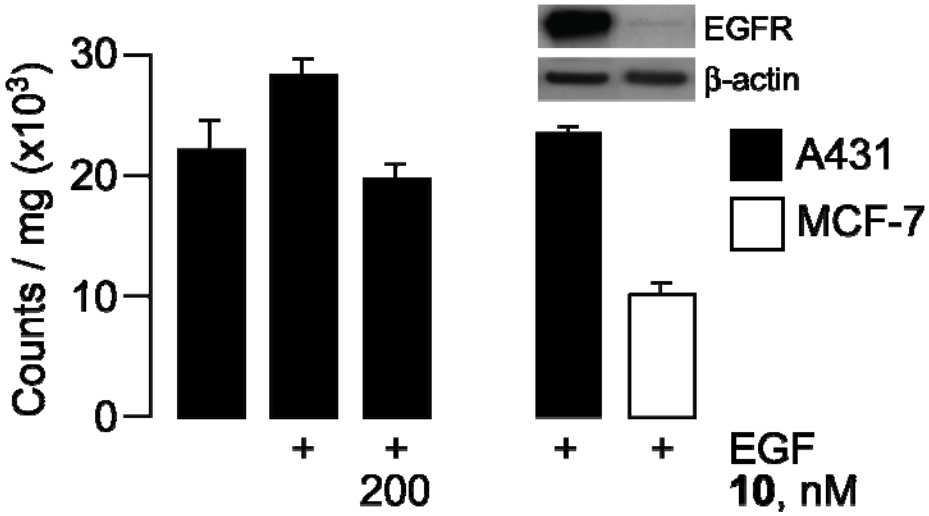

Figure 4. Compound [^{18}F]**17** cell uptake in A431 and MCF-7 cells. Data were expressed as decay-corrected counts per min per mg total cellular protein. Data are mean ± SEM done in triplicate.

Biodistribution, metabolic stability and initial PET imaging.

The 60 minutes tissue biodistribution of [^{18}F]**17** in A431 tumor bearing mice, expressed as tissue to blood ratios, is shown in Figure 5. The radiotracer appeared to be eliminated via both the hepatobiliary and renal routes, as the highest tissue radioactivities were found in gallbladder and urine. Elimination of the radiotracer into the gut may also account for the high radioactivity in early part of the intestine. Low radioactivity was observed in most other organs including muscle and heart. The low uptake in bone suggests that the radiotracer does not undergo defluorination. Tumor (A431 xenograft) uptake was approximately four-fold higher than that of muscle (Figure 5).

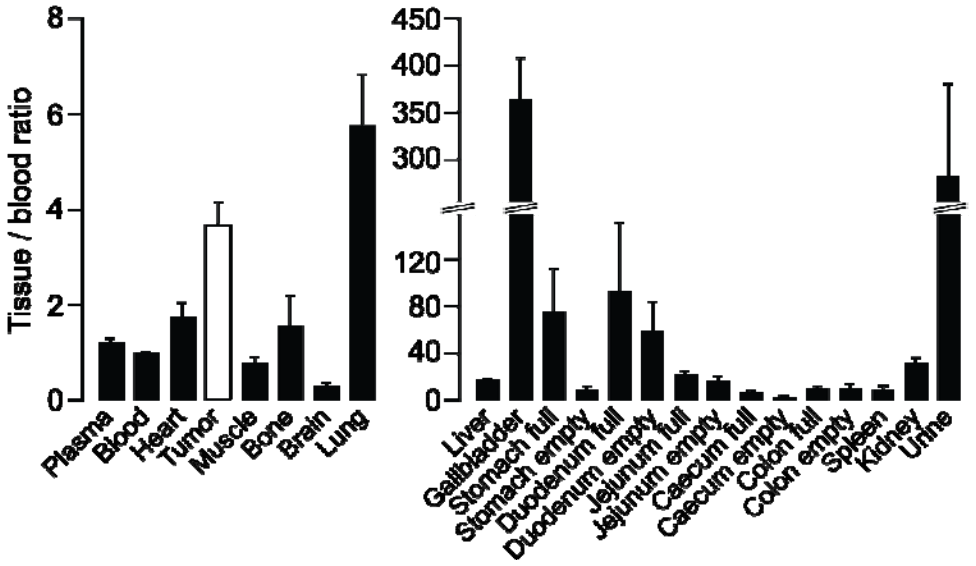

Figure 5. Tissue distribution of compound [^{18}F]**17** in untreated tumor bearing mice at 60 min. Data are ±SEM; n=3 mice.

We investigated the *in vivo* metabolic stability in non-tumor bearing mice by analysing liver and plasma extracts at 2, 30 and 60 minutes post-injection. Sample analysis was accomplished by radio-HPLC. Typical radiochromatograms are shown in Figure 6. At 2 min, only parent

compound was observed in plasma. A more polar radioactive metabolite was seen in plasma at 30 min and similarly one low level metabolite peak was seen in liver. The metabolic stability data, summarized in Table 2, demonstrates that parent radiotracer [^{18}F]**17** remains a major component of both liver and plasma even at 60 minutes post injection; indicative of a relatively good stability *in vivo*.

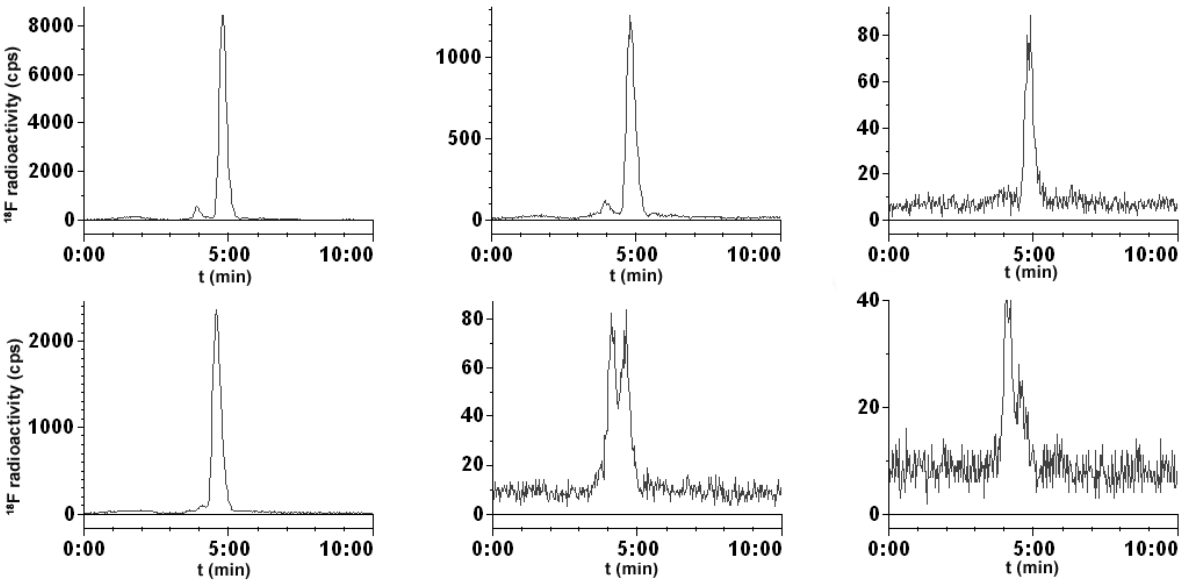

Figure 6. *In vivo* metabolism of compound [^{18}F]**17** in mice as assessed by radio-HPLC. Top panel: 2 min, 30 min and 60 min liver, respectively; Bottom panel: 2 min, 30 min and 60 min plasma, respectively.

Table 2. *In vivo* metabolism of compound [^{18}F]**17** at selected time points, showing the proportion of compound [^{18}F]**17** present in plasma and liver extracts[a].

Time (min)	Parent (Liver)	Parent (Plasma)
2	95.00 ± 1.00	98.92 ± 1.06
30	85.06 ± 1.75	62.81 ± 1.70
60	75.45 ± 2.73	49.75 ± 6.27

[a] The extracts were analyzed by radio-HPLC [50% MeCN (0.085% H_3PO_4)]. The values are the average of 3 independent studies per time point. Proportion of compound [^{18}F]**17** in plasma and liver were calculated by

comparison of compound [^{18}F]**17** peak to total radioactivity present on chromatogram. The efficiency of the extraction from plasma was 83.5%.

We further assessed the potency of compound [^{18}F]**17** to detect an A431 xenograft by small animal PET imaging. A summed image for a dynamic PET scan 30-60 minutes post-injection of [^{18}F]**17** is shown in Figure 7. Tumor uptake is clearly observable; significant radiotracer localization was also seen in the abdominal region.

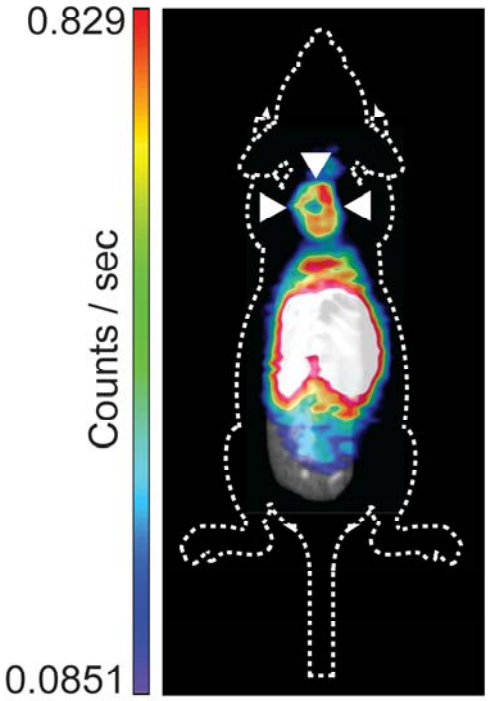

Figure 7. Compound [^{18}F]**17** PET image of one representative A431 xenograft-bearing mouse. White arrowheads indicate the tumor.

Discussion

Previous PET imaging studies with irreversible inhibitors of EGFR[14] showed the importance of having a highly selective and metabolically stable radiotracer to enhance tumor uptake and improve the quality of the imaging. With this in mind, we selected the 3-cyanoquinoline **1** first reported by Tsou *et at*.[28, 31, 44] and introduced a number of subtle chemical modifications into the structure with the aim of retaining high affinity for the EGFR tyrosine kinase. The 3-cyanoquinoline core, as explained earlier, was chosen in preference to the quinazoline core because its interaction with the binding site was expected to be more entropically favored. The 4-dimethylaminocrotonylamide at the C-6 position (the Michael acceptor) was selected because it was expected to be reasonably physiologically stable but display good chemoselectivity towards reaction with the thiol residue of Cys-773 in the kinase active site. Taking into consideration previously reported molecular modeling studies,[28] a small focused library of fluorine containing 3-cyanoquinolines was then synthesized (compounds **1**, **10**, **13**, **14**, **17**, **18**, **24** and **25**) and these compounds tested for their ability to inhibit the intracellular tyrosine kinase autophosphorylation activity of EGFR. The fluorine containing groups were introduced onto both the Michael acceptor moiety and the C-7 ether position of the quinoline core. Previous studies have indicated the tolerance for substitution at these sites, which made the 6- and 7-positions attractive for modification in the present investigation. Neither of these positions was expected to be critical for binding and so it was hoped that the high affinity of the parent compound **1** would be preserved. The synthetic routes developed to prepare these derivatives were designed such that they would be amenable also for the preparation of the corresponding [^{18}F]-fluorine containing congeners from ready available radiolabeled precursors (*i.e.* [^{18}F]-1-fluoro-2-ethyltosylate,[45] [^{18}F]-*p*-fluorobenzaldehyde[46] or [^{18}F]-1-fluoro-2-ethylazide[39]). Although compounds modified at the Michael acceptor were preferred because they could be accessed by a convergent synthetic approach, quinoline **24** was also

synthesized in order to evaluate the affect of modifying the C-7 position on *in vitro* binding affinity for SAR purposes. Eight compounds in total have been screened for their EGFR tyrosine kinase activity inhibition using BPDQ as positive control. The biological screening also included the non-fluorinated quinolines **1**, **10** and **25**; compound **1** was used as a "standard" and compounds **10** and **25** were the potential radiochemical precursors for those fluorinated quinolines most likely to be translated into imaging agents. We assessed these latter compounds to better understand the potential impact of residual impurities in the final formulated radiopharmaceutical. As expected, in the cell free kinase activity inhibition assay, the subnanomolar binding affinity showed by quinolines **1** and **10** is maintained in quinolines **13** and **14** despite the increased bulkiness on the tertiary amine group. Surprisingly the activity of the alkyne-containing quinoline **25** was in the picomolar range, possibly because of secondary interactions of the alkyne group with the binding site of the enzyme, a feature unfortunately not retained in compound **17**. However compound **17** has an IC_{50} in the nanomolar range which should be quite adequate for its use as imaging agent and shows that the fluoroethyl triazole group is well tolerated in this case, this making the "click labeling" to introduce ^{18}F an attractive method. The slightly higher IC_{50} of **18** can be attributable to the replacement of the tertiary amine, which acts as internal base, with the less basic triazole ring. This could affect the outcome of the Michael reaction with Cys 773 as previously highlighted by Tsou *et al.*[31] in compounds bearing imidazole functionality. Finally, quinoline **24**, designed to be a direct analogue of quinoline **10**, but containing a 2-fluoroethoxy group in place of the C-7 ethoxy group, showed the same activity as compound **10** confirming that the C-7 group is not involved in the binding with the EGFR tyrosine kinase enzyme. With these preliminary encouraging results in hand, the library was screened for its ability to inhibit the autophosphorylation process in the human epithelial carcinoma A431 cell line. All the members of the library were active at nanomolar concentrations except for compound **18** and

the positive control BPDQ. Compounds **13**, **14**, **17** and **25** were, however, 10 fold less active than reference compounds **1** and **10**.

The lack of activity of compound **18** might be accounted for by its inability to cross the cell membrane, although from a structural point of view, it is not apparent to us why this would be the case as its physicochemical properties are comparable with the other members of the series. Alternatively, the lack of activity of compound **18** in cells may be a consequence of it having a more reversible interaction with the kinase, as the methodology we employed for measuring cellular activity (with washing steps) permits irreversible inhibition to be quantified. This hypothesis can be reinforced by the lack of activity of BPDQ which is clearly a reversible inhibitor of EGFR. A reversible interaction of compound **18** with EGFR kinase is possible since replacement of the amine group at the terminus of the Michael acceptor with a nitrogen atom contained within a triazole ring system could prevent the Michael reaction of the Cys-773 thiol from occurring; this would result in abolition of activity in the cellular assay. The low basicity of the triazole nitrogen and/or the lack of conformational flexibility of this group could well be preventing the Michael acceptor from reacting efficiently. In particular, the aromatic nature of the triazole ring combined with the sp^2 hybridisation structure of the N-3 atom ensures that its basicity is likely $\sim 10^9$ folds lower than that of the secondary/tertiary amines. Moreover, the triazole ring has an extended planar π-electron system conjugated to the amide carbonyl group and consequently will have a significant barrier to rotation to give the current orientation in which this nitrogen lone pair can assist with general base catalysis of the attack of the Cys 773 thiol at a Bürgi-Dunitz angle to the γ position of the enamide unit.

We interpret the lower activity of **13**, **14**, **17** and **25** relative to **1** and **10** as suggesting that bulkier groups on the amine of the Michael acceptor have a negative effect on the cellular

activity. This effect is particularly apparent for compound **25** whose activity decreases 2000 fold in the cell relative to its activity in the cell-free assay. This may be due to side reactions of the alkyne moiety with the cell surface which could partially prevent its penetration into the cell. Compound **24**, where the Michael acceptor has not been modified, shows comparable activity to compounds **1** and **10**.

Taking these results into consideration, we first selected compound **14** as a potential radioimaging agent despite its high Log*P*, because of its high affinity in the kinase assay and in cells and also because its preparation in radiolabeled form was *via* a reductive amination protocol which we were keen to develop. The synthesis of the [^{18}F]-*p*-fluorobenzaldehyde was performed by displacement of the corresponding *p*-tetramethylamonium benzaldehyde triflate with [^{18}F]KF/Kryptofix. The reductive amination step between [^{18}F]-*p*-fluorobenzaldehyde and the radiochemical precursor **10** was attempted under various reaction conditions (*e.g.* different temperatures, different heating methods and different borohydrides) but it always gave [^{18}F]-*p*-fluorobenzyl alcohol as major product as detected by analytical radio-HPLC. However, as the formation of the intermediate imine seemed to be far slower than the reduction of the fluorobenzaldehyde in all the conditions we examined, we decided to abandon the radiosynthesis of compound **14** and select a different lead compound.

Quinoline **17** was then selected for further development. This compound looked to have an attractive balance between high binding affinity *in vitro*, structural novelty, and a radiosynthesis method that would rely on efficient click-chemistry as developed within the group. Moreover, quinoline **17** displays a lower Log*P* than **14** and it was considered that this could favor its performance as imaging agent. Cognizant of the importance of a favorable metabolic profile for a potential imaging agent, we decided to test compound **17** for its stability in mouse and human liver microsomes in comparison with compound **10**.

Interestingly, after 60 min of incubation, only the parent compound was detected by HPLC (data not shown). The absence of more polar metabolites appears to confirm our expectation that secondary amine substituted Michael acceptors display greater metabolic stability than their tertiary amine analogues.[30] The C-7 ethoxy group also appears to be relatively stable in this regard. The radiosynthesis of [^{18}F]-**17** has been described in detail in the Results section and this compound has been evaluated both *in vitro* and *in vivo*. An initial *in vitro* cell uptake study was performed in a human epithelial carcinoma A431 cell line. The uptake of compound **17** was increased in the presence of EGF stimulation and decreased when the cell was pre-treated with an excess of quinoline **10** used as a blocking agent. This suggested that the effect is specific for EGFR. A further study was designed to compare A431 and MCF-7 cell lines as these present different levels of EGFR expression. As expected from EGFR overexpression in the former cell line, [^{18}F]**17** uptake was higher in A431 than MCF-7 cells. Encouraged by these *in vitro* results we proceeded to carry out a preliminary *in vivo* validation to confirm the metabolic stability of compound **17** and to evaluate the tumor uptake and the PET imaging quality of radiotracer [^{18}F]**17** in mice. Metabolism studies were accomplished by radio-HPLC analysis of plasma and liver samples of non-tumor bearing mice treated with [^{18}F]**17** at three time points (2, 30 and 60 min). After 2 min, only tracer [^{18}F]**17** was detected in plasma while a more polar metabolite appeared after 30 min. Without any further work, we can only speculate that the polar metabolite is a C-7 *O*-de-ethylated product. However tracer **17** looked fairly stable in liver as the parent compound was by far the major component detected after 60 min. The tissue distribution of [^{18}F]**17** at 60 min post injection showed that the radiotracer is probably eliminated via both the hepatobiliary and renal routes. Elimination of the radiotracer into the gut may also account for the high radioactivity in the early part of the intestine. Compared to other radiotracers reported in the literature,[43] [^{18}F]**17** shows reduced kidney, liver and lung uptake which may be related to its

relatively high metabolic stability and also suggests that [^{18}F]**17** may be a more suitable candidate for upper torso imaging. The tumor to muscle ratio of 4:1 compares favorably with data reported in the literature. The low uptake in bone suggests that the radiotracer does not undergo defluorination. As a final investigation, we assessed the potency of compound [^{18}F]**17** to detect a A431 xenograft by small animal PET imaging. Although high non-specific localization was seen in the elimination organs, the uptake into the tumor was clearly visible. These data warrant further investigation of [^{18}F]**17** and other radiotracers of the cyanoquinoline series as EGFR imaging agents.

Conclusions.

We have synthesized a small library of fluorine containing 3-cyanoquinolines and we have screened them for their ability to inhibit the EGFR autophosphorylation process. All the members of the library were active at sub-nanomolar or nanomolar concentration in the cell free EGFR tyrosine kinase assay and in the EGFR overexpressing human epithelial carcinoma A431 cell line. We then selected the lead compound **17** for its transformation into an imaging agent and we developed the radiosynthesis of [^{18}F]**17** by a well established "click chemistry" protocol previously developed within the group. Radiotracer [^{18}F]**17** was evaluated *in vitro* for its ability to trace the EGFR receptor and it looked promisingly selective. A preliminary *in vivo* validation was also carried out. Tracer [^{18}F]**17** looked reasonably metabolically stable and it showed a relative high uptake into the tumor with respect to organs like muscle and heart. An A431 xenograft was clearly imaged by small animal PET scan. All these data highlighted the potential of [^{18}F]**17** as imaging agent and prompt further investigation for its ability to non-invasively assess the EGFR expression/activation *in vivo*. They also encouraged the development of other radioimaging agents based on the 3-cyanoquinoline core.

Experimental Section

Chemistry and radiochemistry: Solvents were distilled as follows: THF and Et_2O over Na-benzophenone ketyl, toluene over Na and CH_2Cl_2 over CaH_2. Reagents were used as commercially supplied unless otherwise stated and handled in accordance with COSHH regulations. Flash chromatography (FC) was carried out on Silica gel (BDH Silica gel for FC) according to the method described by Still. NMR spectra were recorded at 400 MHz on a Bruker AV-400 or Bruker DX-400 instrument or at 500 MHz on a Brucker AV-500 instrument. The frequency of the instruments is related to proton. Chemical shifts (δ) are given in parts per million (ppm) as referenced to the appropriate residual solvent peak. Broad signals are assigned as br. ^{13}C chemical shifts (δ) are assigned as s, d, t, and q, for C, CH, CH_2, and CH_3 respectively. Infrared spectra were recorded as thin films, on Perkin-Elmer Paragon 1000 Fourier transform spectrometer. Only selected absorbances (ν_{max}) are reported. Low resolution and high-resolution mass spectra were recorded on a VG Prospec spectrometer, with molecular ions and major peaks being reported. Intensities are given as percentages of the base peak. HRMS values are valid to ±5 ppm. [^{18}F]Fluoride was produced by a cyclotron (Scanditronix MC40) using the $^{18}O(p,n)^{18}F$ nuclear reaction with 19 MeV proton irradiation of an enriched [^{18}O]H_2O target.

HPLC Methods. (a) Purity analysis of nonradioactive tested compounds was carried out on an Agilent 1200 series system with Laura 4 software (Lablogic, Sheffield, UK) or Beckman System Gold with a Phenomenex Luna 50 mm × 4.6 mm (3 μm) HPLC column attached and a mobile phase as reported in the supporting information. Tested compounds showed a purity ≥ 95%. (b) Preparative radio-HPLC was carried out on a Beckman System Gold equipped with a Bioscan Flowcount FC-3400 PIN diode detector (Lablogic) and a linear UV-200 detector (wavelength 254 nm). A Phenomenex Luna C18 150 mm × 10 mm HPLC column and a

isocratic mobile phase of water and 20% acetonitrile (0.085% H_3PO_4) and flow rate 3 mL/min. (c) Analytical radio-HPLC was carried out as above but using a Bioscan Flowcount FC3200 sodium iodide/PMT gamma detector (Lablogic), a Thermo Spectra SERIES UV150 (wavelength 254 nm), and a Phenomenex Luna 50 mm × 4.6 mm (3 μm) column with an isocratic mobile phase of water and 22% acetonitrile (0.1% TFA), flow rate 1 mL/min.

Synthesis: Compounds **1**, **3**, **4**, **5** and **6** were synthesized accordingly with established literature procedures and ^{1}H-NMR spectral data were consistent with reported values**.**

(*E*)-4-(*tert*-Butoxycarbonyl-prop-2-ynylamino)-but-2-enoic acid methyl ester (**8**): 4-Bromo methylcrotonate (**7**, 1g, 5.6 mmol) was dissolved in dry THF (10 mL) and propargyl amine (961 μL, 14 mmol) was added dropwise at –20 °C. The resulting mixture was stirred at –20 °C for 4 h then cooled to –65 °C. Boc_2O (4.9 g, 22.3 mmol) and Et_3N (4 mL, 27.9 mmol) were then added in turn and the mixture stirred at –65°C→rt for 14 h. The white solid was filtered off and the mother liqueur was concentrated under reduced pressure, dissolved in CH_2Cl_2 (30 mL) and washed with water (20 mL), HCl 1M (20 mL), water (20 mL) and brine (20 mL) and finally dried over $MgSO_4$. The crude residue was purified by chromatography on silica gel (Et_2O /petroleum ether, 1:4; R_f = 0.12) to give the title compound (681 mg, 49%) as colorless oil.

^{1}H NMR (400 MHz, $CDCl_3$) δ 6.90 (dt, J = 15.7, 5.3, 1H), 5.93 (d, J = 15.7, 1H), 4.19-3.91 (m, 4H), 3.77 (s, 3H), 2.24 (t, J = 2.4, 1H), 1.49 (s, 9H); ^{13}C NMR (101 MHz, $CDCl_3$) δ 166.5 (s), 154.6 (s), 143.6 (d), 122.1 (d), 121.8 (d), 81.0 (s), 78.9 (d), 72.3 (s), 71.9 (s), 51.7 (q), 47.0 (t), 46.8 (t), 36.4 and 35.9 (t), 28.3 (q, 3C); IR: ν_{max} 3263, 2976, 2361, 1699, 1450, 1273, 1167 cm^{-1}; MS (ESI): m/z (%) 276 [MNa^+] (35); HR-MS (ESI) Calcd for $C_{13}H_{19}NO_4Na$: 276.1211, found 276.1212 (Δ –0.4 ppm).

***N*-[4-(3-Chloro-4-fluorophenylamino)-3-cyano-7-hydroxyquinolin-6-yl]-acetamide** (**20**): The quinoline **19** (500 mg, 1.15 mmol) was suspended in dry CH_2Cl_2 (50 mL) and BBr_3 (1.0

M in CH_2Cl_2, 5.7 mL, 5.7 mmol) was added dropwise at rt. The mixture was stirred 14 h and quenched with water (20 mL). The yellow precipitate was collected, washed with water (50 mL) and dried under vacuum. The title compound **20** was obtained as a yellow solid (166 mg, 40%) and used in the next step without further purification.

^{1}H NMR (400 MHz, MeOD) δ 9.12 (s, 1H), 8.79 (s, 1H), 7.68 (dd, J = 1.5, 6.1, 1H), 7.51-7.45 (m, 1H), 7.41 (t, J = 8.7, 1H), 7.35 (s, 1H), 2.28 (s, 3H); ^{13}C NMR (101 MHz, MeOD) δ 170.9 (s), 158.2 [s, (d, J_{CF} = 250.0)], 155.6 (s), 154.7 (s), 147.3 (d), 136.4 (s), 134.0 (s), 130.0 (s), 129.4 (d), 127.6 [d, (d, J_{CF} = 7.9)], 121.4 [s, (d, J_{CF} = 19.0)], 117.6 [d, (d, J_{CF} = 22.8)], 113.7 (d), 113.1 (s), 111.4 (s), 102.3 (d), 86.1 (s), 22.7 (q); IR: ν_{max} 3357, 3018, 2925, 2228, 1613, 1539, 1495, 1469, 1238 cm^{-1}; MS (ESI): *m*/*z* (%) 371 [MH^+] (100), 144 (25); HR-MS (ESI) Calcd for $C_{18}H_{13}N_4O_2ClF$: 371.0711, found 371.0707 (Δ –1.1 ppm).

***N*-[4-(3-Chloro-4-fluorophenylamino)-3-cyano-7-(2-fluoro-ethoxy)-quinolin-6-yl]-acetamide (21), 6-Amino-4-(3-chloro-4-fluorophenylamino)-7-(2-fluoroethoxy)-quinoline-3-carbonitrile** (**22**): The quinoline **20** (25 mg, 0.06 mmol) was heated with K_2CO_3 (41.4 mg, 0.30 mmol) and 2-mesyloxy-1-fluoroethane (17 mg, 0.12 mmol) in DMF (1 mL) at 70 °C overnight. The mixture was cooled at rt, water (1 mL) was added and the quinoline **21** (yellow solid, 20 mg, 83 %) was collected, washed with water (3 mL) and diethyl ether (3 mL), dried under vacuum and used without further purification. Compound **21** was refluxed in water (0.5 mL) and conc. HCl (0.5 mL) for 2.5 h then cooled at rt. The crude mixture was concentrated under reduced pressure, dissolved in water (2 mL) and neutralized with K_2CO_3. Quinoline **22** (8 mg, 53 %) was collected as a yellow solid.

^{1}H NMR (400 MHz, MeOD) δ 8.33 (s, 1H), 7.94 (s, 1H), 7.47 – 7.00 (m, 4H), 5.09 – 4.74 (dm, J_{HF} = 54.7, 2H), 4.48 (d, J_{HF} = 28.5, 2H); ^{19}F NMR (376 MHz, MeOD) δ –122.4, –225.1.

General procedure for the synthesis of compounds 9, 11, 12 and 23.

The amino quinolines **6** or **22** (1 eq) and the Michael acceptor **4**, **5** or **8** (1.5 eq) were suspended and sonicated in dry CH_2Cl_2 (0.06 M) and $AlMe_3$ (2.0 M solution in hexane, 2 eq) was added dropwise at rt. The mixture was stirred at rt and monitored by TLC to the disappearance of the starting quinoline. The mixture was quenched with a saturated solution of $NaHCO_3$ and the phases were separated. The aqueous layer was extracted twice with CH_2Cl_2 and the combined organic layers washed with brine and dried over $MgSO_4$. The crude mixture was purified by chromatography on silica gel or plate silica gel TLC.

{(*E*)-3-[4-(3-Chloro-4-fluorophenylamino)-3-cyano-7-ethoxyquinolin-6-ylcarbamoyl]-allyl}-methylcarbamic acid *tert*-butyl ester (**9**): yellow semisolid, 47% yield; R_f = 0.12 (petroleum ether/ AcOEt: 1,2); ^{1}H NMR (400 MHz, $CDCl_3$): δ 9.20 (s, 1H), 8.53 (s, 1H), 8.07 (s, 1H), 7.91 (br s, 1H), 7.31–7.21 (m, 1H), 7.21–7.13 (m, 1H), 7.12–6.88 (m, 3H), 6.15–6.02 (m, 1H), 4.38–4.27 (m, 2H), 4.08 (br s, 2H), 2.98–2.85 (m, 3H), 2.10 (s, 1H), 1.61 (t, J = 6.9 Hz, 3H), 1.53 (s, 9H);^{13}C NMR (101 MHz, $CDCl_3$): δ 164.4 (s), 156.6 [s (d, J_{CF}= 247.8 Hz], 155.6 (s), 152.0 (d), 150.8 (s), 149.4 (s), 147.2 (s), 143.3 and 142.3 (d), 135.7 (s), 127.3 (s), 125.8 (d), 124.3 (d), 123.1 (d), 121.1 [s, (d, J_{CF}= 18.9 Hz), 116.8 (s), 116.4 [d (d, J_{CF}= 22.3 Hz)], 113.1(s), 109.9 and 109.5 (d), 108.4 (d), 88.3 (s), 79.9 (s), 65.0 (t), 49.9 and 49.3 (t), 34.3 (q), 28.2 (q, 3C), 14.4 (q); MS (ESI): *m*/*z* (%) 554 [MH^+] (100); HR-MS (ESI) Calcd for $C_{28}H_{30}ClFN_5O_4$: 554.1970, found 554.1981 (2.0 ppm).

{(*E*)-3-[4-(3-Chloro-4-fluoro-phenylamino)-3-cyano-7-ethoxy-quinolin-6-ylcarbamoyl]-allyl}-prop-2-ynyl-carbamic acid *tert*-butyl ester (**11**): colorless oil; 68% yield, R_f = 0.14 (eluent: AcOEt /Et_2O, 10/1); ^{1}H NMR (400 MHz, $CDCl_3$) δ 9.18 (s, 1H), 8.39 (s, 1H), 8.17 (br s, 1H), 7.96 (s, 1H), 7.08 (s, 1H), 7.05–6.94 (m, 2H), 6.89 (t, J = 8.6, 1H), 6.68 (m, 1H), 6.08 (d, J = 14.9, 1H), 4.22 (q, J = 6.9, 2H), 4.13 (d, J = 4.2, 2H), 4.05 and 3.90 (br s, 2H), 2.25 (t, J = 2.2, 1H), 1.58 (t, J = 7.0, 3H), 1.48 (s, 9H); ^{13}C NMR (101 MHz, $CDCl_3$) δ 164.3 (s), 155.8 [s (d, J_{CF}= 249.8 Hz], 154.7 (s), 152.1 (d), 151.0 (s), 149.6 (s), 147.3 (s), 142.7 and

142.2 (d), 135.7 (s), 127.5 (s), 126.1 (d), 125.5 (d), 123.43 and 123.36 (d), 121.2 [s; (d, J = 18.9)], 116.8 (s), 116.5 [d, (d, J = 22.3)]; 113.2 (s), 109.7 (d), 108.5 (d), 88.5 (d), 81.0 (s), 79.1 (s), 72.2 and 71.9 (d), 65.1 (t), 47.0 (t), 36.5 and 35.9 (t), 28.3 (q; 3C), 14.1 (q); MS (ESI): *m*/*z* (%) 578 [MH^+] (100); IR: ν_{max} 3412, 3307, 2980, 2930, 2252, 2214, 1690, 1682, 1537, 1250, 734 cm^{-1}; HR-MS (ESI) Calcd for $C_{30}H_{30}N_5O_4FCl$: 578.1970, found 578.1948 (Δ –3.8 ppm).

(*E*)-Pent-2-en-4-ynoic acid [4-(3-chloro-4-fluorophenylamino)-3-cyano-7-ethoxy-quinolin-6-yl]-amide (**12**): yellow solid, 20% yield, R_f = 0.13 (Et_2O); ^1H NMR (500 MHz, $CDCl_3$) δ 9.10 (s, 1H), 8.56 (s, 1H), 8.09 (s, 1H), 7.39 (s, 1H), 7.35 (br s, 1H), 7.24 (dd, J = 6.3, 2.7, 1H), 7.16 (t, J = 8.6, 1H), 7.08 (ddd, J = 2.8, 3.9, 8.7, 1H), 6.82 (dd, J = 1.6, 15.4, 1H), 6.55 (d, J = 15.4, 1H), 4.33 (q, J = 7.0, 2H), 3.40 (dd, J = 0.4, 2.4, 1H), 1.76 (br s), 1.58 (t, J = 7.0, 3H); ^{13}C NMR (126 MHz, $CDCl_3$) δ 162.6 (s), 156.6 [s, (d, J_{CF} = 249.0), 152.2 (d), 151.3 (s), 150.0 (s), 147.6 (s), 135.6 (s), 134.2 (d), 128.1 (s), 126.9 (d), 124.6 [d, (d, J_{CF} = 7.1)], 122.9 (d), 121.9 [s, (d, J_{CF} = 19.1)], 117.2 [d, (d, J_{CF} = 22.3)], 116.5 (s), 113.2 (s), 109.9 (d), 108.8 (d), 89.2 (s), 86.3 (d), 80.3 (s), 65.3 (t), 14.5 (q); ^{19}F NMR (376 MHz, CDCl3) δ –117.0 ppm; IR: ν_{max} 3300, 2925, 2361, 2342, 2214, 1670, 1624, 1539, 1498, 1458, cm^{-1}; MS (ESI): *m*/*z* (%) 435 [MH^+] (100); HR-MS (ESI) Calcd for $C_{23}H_{17}N_4O_2FCl$: 435.1024, found 435.1018 (Δ –1.4ppm).

{(*E*)-3-[4-(3-Chloro-4-fluoro-phenylamino)-3-cyano-7-(2-fluoroethoxy)-quinolin-6-ylcarbamoyl]-allyl}-methylcarbamic acid *tert*-butyl ester (**23**): yellow oil, 61 % yield; R_f = 0.38 (AcOEt); ^1H NMR (500 MHz, $CDCl_3$) δ 9.15 (s, 1H), 8.57 (s, 1H), 8.10 (s, 1H), 7.40 (s, 1H), 7.31–7.25 (m, 1H), 7.21 – 7.14 (m, 1H), 7.14 – 7.07 (m, 1H), 6.93 (dt, J = 5.0, 15.2, 1H), 6.13 – 5.98 (m, 1H), 4.90 (dm, J_{HF} = 47.9, 2H), 4.50 (dm, J_{HF} = 27.3, 2H), 4.06 (br s, 2H), 2.91 (br s, 3H), 1.91 (br s, 1H), 1.48 (s, 9H); ^{13}C NMR (126 MHz, $CDCl_3$) δ 163.6 (s), 156.6 [s, (d, J_{CF} = 284.1)], 155.8 (s), 152.3 (d), 150.6 (s), 150.0 (s), 147.1 (s), 142.6 and 142.2 (d),

135.5 (s), 128.4 (s), 126.9 (d), 124.6 (d), 123.5 (d), 121.8 [s, (d, J_{CF} = 19.6)], 117.2 [d, (d, J_{CF} = 22.3)], 116.5 (s), 113.8 (s), 110.0 (d), 109.2 (d), 100.0 (s), 85.4 [t (d, J_{CF} = 174.1)], 80.9 (s), 68.4 [t (d, J_{CF} = 19.5)], 50.0 and 49.4 (t), 34.6 and 34.5 (q), 29.7 (s, 3C); MS (ESI): *m*/*z* (%); 572 [MH^+] (100); HR-MS (ESI) Calcd for $C_{28}H_{29}N_5O_4ClF_2$: 572.1876, found 572.1868 (Δ – 1.4 ppm).

General procedure for the synthesis of compounds 10, 17, 24 and 25.

Quinoline **9**, **11**, **Boc-17** or **23** (1 eq) were dissolved in 1,4-dioxane (0.03 M) and conc. HCl (0.003 M) was added dropwise at rt. The mixture was stirred 30 min – 1 h and the precipitate was collected and washed with dioxane and diethyl ether and dried under vacuum to give the title compounds as HCl salts.

(*E*)-4-(Methylamino)-but-2-enoic acid [4-(3-chloro-4-fluorophenylamino)-3-cyano-7-ethoxyquinoline-6-yl] amide hydrochloride (**10·HCl**): yellow solid; 78% yield; ^{1}H NMR (400 MHz, MeOD): δ 9.24 (s, 1H), 8.87 (s, 1H), 7.72 (dd, *J* = 6.5, 2.5 Hz, 1H), 7.52 (ddd, *J* = 6.5, 8.7, 2.5, 1H), 7.48–7.36 (m, 2H), 7.00 (dt, , *J* = 15.2, 1H), 6.82 (dt, *J* = 15.2, 1.4, 1H), 4.47 (q, *J* = 7.0, 2H), 3.92 (d, *J* = 6.4, 2H), 2.78 (s, 3H), 1.62 (t, *J* = 7.0, 3H); ^{13}C NMR (101 MHz, MeOD): δ 163.5 (s), 158.1 [s (d, J_{CF}= 250.1 Hz], 155.7 (s), 154.5 (s), 147.5 (d), 146.1 (s), 136.6 (s), 134.6 (d), 133.8 (s), 129.6 (d), 129.4 (d), 127.7 [d (d, J_{CF}= 7.8 Hz)], 121.3 [s (d, , J_{CF} = 19.2)], 117.0 [d (d, J_{CF}= 22.7 Hz)], 114.0 (d), 113.1 (s), 111.9 (s), 100.3 (d), 86.7 (s), 66.8 (t), 48.9 (t), 32.2 (q), 13.2 (q); MS (ESI): *m*/*z* (%) 454 [MH^+] (48), 248 (100); HR-MS (ESI) Calcd for $C_{23}H_{22}ClFN_5O_2$: 454.1446, found 454.1459 (2.9 ppm).

(*E*)-4-Methylamino-but-2-enoic acid [4-(3-chloro-4-fluorophenylamino)-3-cyano-7-(2-fluoroethoxy)-quinolin-6-yl]-amide hydrochloride (**24**): yellow solid; 67 % yield; ^{1}H NMR (400 MHz, MeOD) δ 9.27 (s, 1H), 8.93 (br s, 1H), 7.73 (dd, *J* = 6.5, 2.5, 1H), 7.55 – 7.48 (m, 2H), 7.48 – 7.40 (m, 1H), 7.01 (dt, *J* = 15.1, 6.5, 1H), 6.83 (d, *J* = 15.4, 1H), 5.06 – 4.87 (dm, 2H), 4.67 (dm, *J* = 28.7, 2H), 3.93 (d, *J* = 6.5, 2H), 2.79 (s, 3H); ^{19}F NMR (376 MHz, MeOD)

δ –118.1, –223.9; ^{13}C NMR (101 MHz, MeOD) δ 164.8 (s), 159.7 [s, (d, J_{CF} = 255.2)], 156.9 (s), 156.2 (s), 149.55 (d), 138.6 (s), 135.5 (d), 135.3 (s), 131.2 (d), 131.0 (s), 130.8 (d), 128.9 [d, (d, J_{CF} = 7.9)], 122.9 [s, (d, J_{CF} = 19.3)], 118.6 [d, (d, J_{CF} = 22.8)], 116.2 (d), 114.4 (s), 113.8 (s), 102.5 (d), 101.9 (s), 82.7 [t (d, J_{CF} = 169.7)], 71.0 [t, (d, J_{CF} = 19.8)], 50.2 (t), 33.3 (q); MS (ESI): *m*/*z* (%); 472 [MH^+] (52), 257 (100); HR-MS (ESI) Calcd for $C_{23}H_{21}N_5O_2ClF_2$: 472.1354, found 472.1342 (Δ –2.1 ppm).

(*E*)-4-Prop-2-ynylaminobut-2-enoic acid [4-(3-chloro-4-fluorophenylamino)-3-cyano-7-ethoxy-quinolin-6-yl]-amide hydrochloride (**25**): yellow solid; 99% yield; ^{1}H NMR (400 MHz, d_6-DMSO) δ 11.02 (br s, 1H), 9.98 (s, 1H), 9.83 (s, 2H), 9.14 (s, 1H), 8.98 (s, 1H), 7.75 (d, *J* = 6.6, 1H), 7.61–7.57 (m, 1H), 7.55 (t, *J* = 8.5, 1H), 7.50 – 7.44 (m, 1H), 6.90–6.78 (m, 1H), 6.81 (t, *J* = 11.9, 1H), 4.36 (q, *J* = 7.0, 2H), 3.95 (s, 2H), 3.87 (d, *J* = 5.4, 2H), 3.76 (t, *J* = 2.3, 1H), 1.50 (t, *J* = 6.9, 3H); ^{13}C NMR (101 MHz, d_6-DMSO) δ 162.8 (s), 156.3 [s, (d, J_{CF} = 247.0)], 155.2 (s), 153.2 (s), 149.3 (d), 139.6 (s), 135.4 (s), 134.3 (d), 129.6 (d), 128.6 (d), 127.9 (s), 126.7 [d (d, J_{CF} = 7.0)], 119.9 [s (d, J_{CF} = 18.9)], 117.4 [d, (d, J_{CF} = 22.3)], 116.3 (d), 114.7 (s), 112.5 (s), 102.9 (d), 86.9 (s), 79.8 (d), 74.8 (s), 65.4 (t), 46.2 (t), 35.3 (t), 14.1 (q); MS (ESI): *m*/*z* (%) 478 [MH^+] (100); HR-MS (ESI) Calcd for $C_{25}H_{22}N_5O_2FCl$: 478.1446, found 478.1448 (Δ 0.4 ppm).

(*E*)-4-{[1-(2-Fluoro-ethyl)-1*H*-[1,2,3]triazol-4-ylmethyl]-amino}-but-2-enoic acid [4-(3-chloro-4-fluoro-phenylamino)-3-cyano-7-ethoxy-quinolin-6-yl]-amide hydrochloride (**17**): yellow solid; 99%; ^{1}H NMR (500 MHz, d_6-DMSO) δ 10.99 (br s, 1H), 9.93 (s, 1H), 9.83 (s, 1H), 9.12 (br s, 1H), 8.97 (s, 1H), 8.33 (s, 1H), 7.72 (d, *J* = 6.1, 1H), 7.61 (s, 1H), 7.53 (t, *J* = 9.0, 1H), 7.47-7.41 (m, 1H), 6.87 (dt, *J* = 15.5, 6.35, 1H), 6.78 (d, *J* = 15.6, 1H), 4.84 (dm, *J* = 32.3, 2H), 4.79-4.74 (m, 2H), 4.34 (q, *J* = 7.0, 2H), 4.29 (t, *J* = 4.9, 2H), 3.86 (br dd, *J* = 11.6, 5.9, 2H), 1.49 (t, *J* = 7.0, 3H).; ^{19}F NMR (376 MHz, d_6-DMSO) δ –117.9, –222.0; ^{13}C NMR (101 MHz, d_6-DMSO) δ 162.7 (s), 155.3 [s (d, J_{CF} = 422.7)] 155.1 (s), 154.9 (s), 149.3

(d), 138.5 (s), 135.6 (s), 134.6 (d), 129.4 (d), 128.6 (s), 127.8 [d (d, J_{CF} =7.5)], 126.6 (s), 126.0 (d), 119.8 [s, (d, J_{CF} = 18.9)], 117.3 [d, (d, J_{CF} = 22.3)], 116.4 (d), 114.8 (s), 112.5 (s), 102.9 (d), 86.9 (s), 81.9 [t, (d, J_{CF} = 168.3)], 65.3 (t), 50.2 [t, (d, J_{CF} = 19.4)], 46.6 (t), 40.8 (t), 14.1 (q); MS (ESI): *m*/*z* (%) 567 [MH^+] (80), 440 (100); HR-MS (ESI) Calcd for $C_{27}H_{26}N_8O_2F_2Cl$: 567.1835, found 567.1841 (Δ 1.1 ppm).

(*E*)-4-(Methylamino)-but-2-enoic acid [4-(3-chloro-4-fluorophenylamino)-3-cyano-7-ethoxy-quinoline-6-yl] amide (**10**): The quinoline hydrochloride **10·HCl** (39.0 mg, 0.08 mmol) was dissolved in water (1 mL) and K_2CO_3 (55 mg, 0.4 mmol) was added. The mixture was stirred 14 h at rt and the pale yellow precipitate was collected, washed with water and dried under vacuum to give the title compound **10** (27.1 mg, 78%) as a yellow solid.

^{1}H NMR (400 MHz, MeOD): δ 8.96 (s, 1H), 8.48 (s, 1H), 7.48–7.41 (m, 1H), 7.41–7.35 (m, 1H), 7.35–7.24 (m, 2H), 7.04 (dt, *J* = 15.4, 5.8 Hz, 1H), 6.50 (dt, *J* = 15.5, 1.5 Hz, 1H), 4.37 (q, *J* = 6.8 Hz, 2H), 3.44 (dd, *J* = 5.7, 1.0 Hz, 2H), 2.45 (s, 3H), 1.59 (t, *J* = 6.9 Hz, 3H);

(*E*)-4-[(2-Fluoroethyl) methyl amino]-but-2-enoic acid [4-(3-chloro-4-fluorophenylamino)-3-cyano-7-ethoxyquinoline-6-yl] amide (**13**): Quinoline **10** (32 mg, 0.07 mmol) was dissolved in dry CH_2Cl_2 (0.7 mL) and 1-fluoro-2-mesyloxy ethane (**15**, 13 mg, 0.09 mmol) and Et_3N (20 μL, 0.14 mmol) were added in turn. The mixture was stirred overnight, concentrated and directly purified by preparative silica TLC on silica gel (CH_2Cl_2/MeOH, 20:1; R_f = 0.28) to give quinoline **13** (11.5 mg, 33%) as a yellow solid.

^{1}H NMR (400 MHz, $CDCl_3$): δ 9.17 (s, 1H), 8.54 (s, 1H), 8.11 (s, 1H), 7.53 (s, 1H), 7.33 (s, 1H), 7.21 (dd, *J* = 6.3, 2.6, 1H), 7.12 (t, *J* = 8.6, 1H), 7.08–6.99 (m, 2H), 6.27 (dt, *J* = 15.2, 1.6, 1H), 4.59 (dt, *J* = 47.6, 4.8, 1H), 4.32 (q, *J* = 7.0, 2H), 3.33 (dd, *J* = 5.6, 3.1, 2H), 2.77 (dt, *J* = 28.0, 4.8, 2H), 2.39 (s, 3H), 1.60 (t, *J* = 7.0, 3H); ^{13}C NMR (126 MHz, $CDCl_3$): δ 164.0 (s), 156.4 [s (d, J_{CF}= 248.7 Hz)], 152.2 (d), 151.2 (s), 149.9 (s), 147.4 (s), 143.9 (d),

135.7 (s), 128.3 (s), 126.7 (d), 125.3 (d), 124.3 [d (d, J_{CF}= 7.3 Hz)], 121.7 [s, J_{CF}= 19.0)], 117.1 (s), 116.8 [d (d, J_{CF}= 24.8 Hz)], 113.3 (s), 109.4 (d), 108.8 (d), 88.9 (s), 82.1 [t, (d, J_{CF}= 168.0 Hz)], 65.2 (t), 58.6 (t), 57.0 [t, (d, J_{CF}= 19.7 Hz)], 42.9 (q), 14.5 (q); ^{19}F NMR (376 MHz, $CDCl_3$): δ –117.5, –219.4; MS (ESI): *m*/*z* (%) 500 [MH^+] (76), 271 (100); IR: ν_{max} 3250, 2924, 2212, 1685, 1622, 1537, 1498, 1458, 1393, 1215 cm^{-1}; HR-MS (ESI) Calcd for $C_{25}H_{25}N_5O_2F_2Cl$: 500.1665, found 500.1662 (Δ –0.6 ppm).

(*E*)-4-[(4-Fluorobenzyl) methylamino]-but-2-enoic acid [4-(3-chloro-4-fluorophenylamino)-3-cyano-7-ethoxyquinoline-6-yl] amide (**14**): Quinoline **10** (50 mg, 0.10 mmol) was suspended in dichloroethane (0.3 mL) and *p*-fluorobenzaldehyde (12 μL, 0.11 mmol) and acetic acid (10 μL) were added dropwise at rt. After 30 min, $NaBH(OAc)_3$ (32 mg, 0.15 mmol) was added and the mixture was stirred 14 h at rt. The mixture was quenched with a saturated solution of $NaHCO_3$ (1 mL) and extracted with CH_2Cl_2 (3×2 mL). The combined organic layers were dried over $MgSO_4$. After purification by plate silica TLC (CH_2Cl_2/MeOH, 20:1; R_f = 0.37), the title compound **14** was obtained (12 mg, 21%) as a yellow solid.

^{1}H NMR (400 MHz, $CDCl_3$): δ 9.18 (s, 1H), 8.52 (s, 1H), 8.07 (s, 1H), 7.66 (s, 1H), 7.34–7.27 (m, 4H), 7.12 (dd, *J* = 6.3, 2.5, 1H), 7.12–7.00 (m, 4H), 6.96 (dt, *J* = 8.3, 3.4, 1H), 6.24 (dt, *J* = 15.3, 1.6, 1H), 4.32 (q, *J* = 7.0, 2H), 3.53 (s, 2H), 3.23 (dd, *J* = 5.7, 1.0, 2H), 2.25 (s, 3H), 1.61 (t, *J* = 6.7, 3H); ^{13}C NMR (126 MHz, $CDCl_3$): δ 163.9 (s), 162.1 [s, J_{CF}= 245.1 Hz], 156.5 [s (d, J_{CF}= 249.2 Hz], 152.1 (d), 151.2 (s), 149.8 (s), 147.5 (s), 144.5 (d), 135.7 (s), 134.2 (s), 130.3 [d, (d, J_{CF}= 7.8 Hz, 2C)], 128.5 (s), 126.8 (d), 125.2 (d), 124.3 [d (d, J_{CF}= 7.4 Hz)], 121.6 [s, (d, J_{CF}= 21.0)], 117.2 (s), 116.9 [d (d, J_{CF}= 43.3 Hz)], 115.2 [d (d, J_{CF}= 21.4 Hz, 2C)], 113.3 (s), 109.3 (d), 108.8 (d), 89.1 (s), 65.2 (t), 61.3 (t), 57.8 (t), 42.5 (q), 14.6 (q); ^{19}F NMR (376 MHz, $CDCl_3$): δ–117.6, –115.5; MS (ESI): *m*/*z* (%) 562 [MH^+] (50), 454

(100); IR: ν_{max} 3380, 2922, 2220, 1680, 1620, 1537, 1458 cm^{-1}; HR-MS (ESI) Calcd for $C_{30}H_{27}N_5O_2F_2Cl$: 562.1821, found 562.1828 (1.2 ppm).

General procedure for the synthesis of compounds Boc-17 and 18: Quinoline **11** or **12** (1 eq) was dispersed in water (0.15 M) and fluoro ethylazide **16** (0.5 M solution in DMF, 2 eq), $CuSO_4$ (0.3 eq) and Cu powder (0.3 eq) were added. The mixture was heated by microwave irradiation at 125 °C for 15 min and diluted with water and AcOEt. The phases were separated and the aqueous phase was extracted with AcOEt. The combined organic layers were dried over $MgSO_4$. The crude residue was purified by chromatography on silica gel to give the compounds **Boc-17** or **18** respectively.

{(*E*)-3-[4-(3-Chloro-4-fluorophenylamino)-3-cyano-7-ethoxyquinolin-6-ylcarbamoyl]-allyl}-[1-(2-fluoroethyl)-1*H*-[1,2,3]triazol-4-ylmethyl]-carbamic acid *tert*-butyl ester (**Boc-17**): yellow semisolid; 19% yield; R_f = 0.36 (eluent: AcOEt/MeOH, 10:1); ^{1}H NMR (400 MHz, $CDCl_3$) δ 9.15 (s, 1H), 8.58 (s, 1H), 8.14 (s, 1H), 7.73 (dd, *J* = 5.7, 3.3, 1H), 7.53 – 7.42 (m, 2H), 7.31 (dd, *J* = 6.2, 2.6, 1H), 7.21 (t, *J* = 8.5, 1H), 7.17 – 7.11 (m, 1H), 6.97 – 6.87 (m, 1H), 6.26 – 6.06 (m, 1H), 4.81 (dt, *J*= 46.8, 4.3, 2H), 4.69 (dm, *J* = 26.7, 2H), 4.58 – 4.50 (m, 2H), 4.42 – 4.34 (m, 2H), 4.22 – 4.13 (m, 2H), 1.63 (t, *J* = 6.8, 3H), 1.28 (s, 9H); ^{19}F NMR (376 MHz, $CDCl_3$) δ –59.9, –115.8; ^{13}C NMR (126 MHz, $CDCl_3$) δ 171.1 (s), 163.7 (s), 156.3 [s (d, J_{CF} = 249.0)], 152.1 (d), 151.3 (s), 149.9 (s), 147.3 (s), 145.2 and 144.9 (s), 142.2 and 141.8 (d), 135.6 (s), 128.2 (s), 126.7 (d), 124.4 (d), 124.3 [d (d, J_{CF} = 6.8)], 123.8 and 123.0 (d), 121.6 [s (d, J_{CF} = 19.1)], 117.0 [d (d, J_{CF} = 22.4)], 116.6 (s), 113.2 (s), 109.7 (d), 108.6 (d), 88.9 (s), 81.4 [t (d, J_{CF} = 162.1)], 80.8 (s), 65.2 (t), 50.5 [t (d, J_{CF} = 20.4)], 47.9 and 47.5 (t), 42.0 and 41.5 (t), 28.3 (q, 3C), 14.5 (q); IR: ν_{max} 2925, 2854, 2220, 1688, 1537, 1459, 1163 cm^{-1}; MS (ESI): *m*/*z* (%) 689 [MNa^+] (100), 667 [M^+]; HR-MS (ESI) Calcd for $C_{32}H_{34}N_8O_4F_2Cl$: 667.2360, found 667.2354 (Δ –0.9 ppm).

(*E*)-*N*-[4-(3-Chloro-4-fluorophenylamino)-3-cyano-7-ethoxyquinolin-6-yl]-3-[1-(2-fluoro-ethyl)-1*H*-[1,2,3]triazol-4-yl]-acrylamide (**18**): yellow solid; 32% yield; R_f = 0.28 (AcOEt/MeOH, 1:1); ^{1}H NMR (500 MHz, $CDCl_3$) δ 9.20 (s, 1H), 8.55 (s, 1H), 8.26 (s, 1H), 7.83 (s, 1H), 7.68 (d, *J* = 15.3, 1H), 7.48 (s, 1H), 7.29 (dd, *J* = 6.2, 2.6, 1H), 7.18 (t, *J* = 8.6, 1H), 7.15 – 7.09 (m, 1H), 7.05 (d, *J* = 15.3, 1H), 4.84 (dm, *J* = 46.7, 2H), 4.73 (dm, *J* = 27.1, 2H), 4.35 (q, *J* = 7.0, 2H), 1.61 (t, *J* = 7.0, 3H); ^{19}F NMR (376 MHz, $CDCl_3$) δ –116.1, –220.7; ^{13}C NMR (126 MHz, $CDCl_3$) δ 163.89 (s), 156.73 [s, (d J_{CF} = 250.1), 151.62 (d), 151.38 (s), 150.29 (s), 148.88 (s), 143.57 (s), 135.41 (s), 130.30 (d), 128.75 (s), 127.08 (d), 124.92 (d), 124.72 [d (d, J_{CF} = 6.4)], 122.24 (d), 121.91 [s (d, J_{CF} = 18.9)], 117.23 [d (d, J_{CF} = 22.4)], 116.29 (s), 113.17 (s), 109.54 (d), 108.05 (d), 99.96 (s), 81.36 [t (d, J_{CF} = 173.0)], 65.49 (t), 50.73 [t (d, J_{CF} = 20.5,)], 14.61 (q); IR: ν_{max} 3266, 2954, 2212, 1623, 1538, 1498, 1460, 1224, 1036 cm^{-1}; MS (ESI): *m*/*z* (%) 524 [MH$^+$] (100); HR-MS (ESI) Calcd for $C_{25}H_{21}N_7O_2F_2Cl$: 524.1413, found 524.1404 (Δ –1.7 ppm).

Radiochemistry.

Under an atmosphere of nitrogen, a buffered solution (sodium phosphate buffer, pH 6.0, 250 mM) of sodium ascorbate (50 μL, 8.7 mg, 43.2 μmol) was added to a Wheaton vial (3 mL) containing an aqueous solution of copper(II) sulfate (50 μL, 1.7 mg pentahydrate, 7.0 μmol). After one min, a solution of alkyne **25** (2.1 mg, 4.4 μmol) in MeCN/water, 1:1 (50μL) was added followed by distilled [^{18}F]-2-fluoroethylazide (94-740 MBq) in acetonitrile (100 μL). The mixture was heated at 80 °C for 15 min, the HPLC mobile phase [21% MeCN (0.085% H_3PO_4), 500 μL] was added and the resulting mixture was purified by preparative radio-HPLC. The isolated HPLC fraction was diluted with water (5 mL) and loaded onto a SepPak C18-light cartridge (Waters) that had been conditioned with ethanol (5 mL) and water (10 mL). The cartridge was subsequently flushed with water (5 mL) and [^{18}F]**17** eluted with

ethanol (0.1 mL fractions). The product fraction was diluted with PBS to provide an ethanol content of 10-20% (v/v).

EGFR Tyrosine Kinase Enzyme Inhibition assay.

The inhibitory activity of quinolines **1**, **10**, **13**, **14**, **17**, **18**, **24** and **25** against EGFR kinase activity was measured by a time resolved fluorescence assay (DELFIA, Perkin-Elmer Life Sciences, Boston, MA, USA). The compounds were dissolved in DMSO and diluted in DMSO to give final concentrations of 0.0001 to 100000 μg/mL. EGFR protein (E-3641, Sigma) was incubated with the compounds in a kinase buffer for 15 min at rt in accordance with manufacturer's instructions (DELFIA Tyrosine kinase kit; PerkinElmer). After 15 min at rt the kinase reaction was initiated by addition of 25 μM ATP, 25 mM $MgCl_2$, and 0.25μM/L of biotinylated poly(Glu, Ala, Tyr) in 10 mM HEPES buffer, pH 7.4. The reaction proceeded at rt for 1 h and was stopped by addition of 100 mM EDTA. The enzyme reaction solution was diluted and aliquots added to 96-well ELISA streptavidin plates with shaking for 1 h. The plates were washed and phosphorylated Tyrosine was detected with Eu-labelled antiphosphotyrosine antibody (50 ng/well; PT66; PerkinElmer). After washing and enhancement steps, the plates were assessed in a Victor^3 multi-label counter (PerkinElmer) using the EGFR Europium protocol. The concentration of compound that inhibited 50% of receptor phosphorylation activity (IC_{50}) was estimated by non-linear regression analysis using GraphPad Prism (Version 4.0 for Windows, GraphPad Software, San Diego California USA).

Protein immunoblotting.

The ability of the compounds to diffuse into cells and to inhibit EGFR was assessed by measuring inhibition of receptor phosphorylation by quinolines **1**, **10**, **13**, **14**, **17**, **18**, **24** and **25** in A431 human epidermoid cancer cells (American Type Culture Collection, Manassas, VA, USA). The cells were maintained in DMEM (Sigma-Aldrich Company Ltd, Dorset, UK)

supplemented with 10% fetal bovine serum (Lonza, UK), and 2mM L-glutamine, 100U/ml penicillin, 100μg/mL streptomycin and 1μg/mL fungizone (GIBCO) in 6 well plates incubated at 37 °C in a humidified incubator with 5% CO_2. The experiments were designed to assess irreversibility of EGFR inhibition by the compounds. Cells in exponential growth were incubated with quinolines **1**, **10**, **13**, **14**, **17**, **18**, **24** and **25** at various concentrations for 3 h. EGF (100 ng/ml) was added to the cells during the last 15 min to induce p-EGFR. The medium was removed and replaced with fresh compound-free medium for 1 h. The last step was then repeated twice. The cells were then washed with cold PBS and lysed in RIPA buffer (Invitrogen Ltd, Paisley, UK) supplemented with protease and phosphatase inhibitor cocktails (Sigma-Aldrich Company Ltd, Dorset, UK). Lysates were clarified by centrifugation. The following antibodies were used: rabbit polyclonal antibody anti-p-EGFR (Cell signalling Technology, Denver, MA; 1:1000) and rabbit polyclonal antibody anti-EGFR (Santa Cruz Biotechnology, Santa Cruz, CA; 1:1000) and mouse monoclonal antibody anti-β-actin (Abcam, UK; 1:10000) as primary antibodies. The secondary antibodies were Goat anti-Rabbit IgG HRP (Santa Cruz Biotechnology Santa Cruz, CA; 1:2000) and Goat anti-Mouse IgG HRP (Autogen Bioclear, UK; 1:2000).

***In vitro* cell uptake of radiotracer [^{18}F]17.**

The cellular uptake of radiotracer [^{18}F]**17** was assessed in A431 cells. Cells were cultured in 6-well plates (n = 3) in full growth medium until they reached approximately 80% confluence. The cells were cultured in serum free medium 24 h and 100 ng/mL EGF or corresponding vehicle was added 15 min before [^{18}F]**17** incubation. For one set of studies, the cells were also incubated with 200 nM quinoline **10** for 13 min prior to addition of radiotracer. Furthermore, all cells were pre-treated with 100 μM verapamil 5 min prior the addition of radiotracer [^{18}F]**17**. Radiotracer [^{18}F]**17** was added to each well (~0.37 MBq in

100µL; ~15 GBq/µmol specific radioactivity) and incubated for 1 h at 37°C. The cells were washed 3 times with ice-cold PBS and lysed in RIPA buffer. Aliquots of the lysates were transferred in counting tubes and fluorine-18 radioactivity was immediately determined using a Packard Cobra II gamma counter (PerkinElmer, UK). BCA Protein assay (Pierce, UK) was performed for all samples and data are normalized and expressed as counts/mg of protein.

***In Vivo* PET imaging and biodistribution**.

A431 xenografts were established by s.c. injection of $5x10^6$ cells on the back of 6- to 8-week-old female *nu/nu* Balb/c mice (Harlan). All animal work was performed by licensed investigators in accordance with the United Kingdom's "Guidance on the Operation of Animals (Scientific Procedures) Act 1986" (HMSO, London, United Kingdom, 1990). When tumors reached ~100 mm^3, animals (n = 3) were scanned on a dedicated small animal CT/PET scanner (Siemens Multimodality Inveon, Siemens Molecular Imaging Inc., Knoxville, USA) following a bolus i.v. injection of 3.7 MBq of [^{18}F]**17**. Dynamic emission scans were acquired in list-mode format over 60 minutes. Cumulative images of the dynamic data (30 to 60 min) were iteratively reconstructed (OSEM3D) and used for visualization of radiotracer uptake with the Siemens Inveon Research Workplace software. Direct [^{18}F]**17** tissue biodistribution was assessed subsequent to the PET scan. For this, mice were sacrificed by exsanguination via cardiac puncture under general anesthesia (isofluorane inhalation) and tissues were excised, weighted and immediately counted for fluorine-18 radioactivity on a Cobra II Auto-Gamma counter (Packard Instruments, Meriden, CTA). Data were expressed as tumor to blood ratio.

Metabolism Studies

Non-tumor-bearing mice were injected intravenously with 3.7 MBq of radiotracer [^{18}F]**17**. Plasma and liver were collected at the indicated time and were snap-frozen in liquid nitrogen for subsequent HPLC analysis. For extraction, ice cold MeOH (1.5 mL) was added to plasma. The mixture was centrifuged (15493 × *g*, 4 °C, 3 min) and the resulting supernatant was evaporated to dryness under vacuum at 40 °C using a rotary evaporator. Liver samples were homogenized with ice cold MeOH (1.5 mL) using an IKA Ultra-Turrax T-25 homogenizer prior to centrifugation. The supernatant was then decanted and evaporated to dryness. The samples were re-suspended in HPLC mobile phase (1.2 mL) and filtered through a Whatman PTFE syringe filter (0.2 μm). The samples (1 mL) were analyzed by radio-HPLC on an Agilent 1100 series HPLC system (Agilent Technologies, Stockport, UK) equipped with a *γ*-RAM model 3 gamma-detector (IN/US Systems Inc., Florida) and the Laura 3 software.

The stationary phase comprised of a Waters μBondapak C18 reverse-phase column (300 mm × 7.8 mm) and the mobile phase comprised of water (0.085% H_3PO_4)/acetonitrile (0.085% H_3PO_4) (50:50) running in isocratic mode at a flowrate of 3 mL/min.

Extraction Efficiency for plasma

To pre-weighed counting tubes (n = 4) Dulbecco's phosphate buffered saline (Sigma, Gillingham, UK) (200 μL) was added and to a further set of tubes (n = 4) mouse plasma extract (Mouse plasma lithium heparin - CD-1- Mixed Gender , pooled, Sera Laboratories International, West Sussex, UK) (200 μL) was added and the samples stored on ice until radiopharmaceutical addition. Formulated radiotracer [^{18}F]**17** was added to a set (n = 4) of blank counting tubes and to the tubes containing PBS or plasma. The samples were then incubated at 37 °C for 30 minutes and then snap frozen using dry ice. Immediately prior to extraction samples were thawed on ice and ice-cold methanol (1.5 mL) added. The samples

were then centrifuged (15493 × *g*, 4 °C, 3 minutes). The supernatant was then decanted and evaporated to dryness. The sample was then re-suspended in HPLC mobile phase (1.1 mL) and filtered (Whatman PTFE 0.2 μm, 13 mm filters). Total radioactivity for each sample (control -100%-, PBS extract -95.4%- and plasma extract – 83.5%-) was then measured on a Cobra-II Gamma Counter.

Acknowledgments

This work was funded by Cancer Research UK programme grant C2536/A7602 and UK Medical Research Council core funding grant U.1200.02.005.00001.01.

Supporting Information Available: Tables of purity data and further HPLC chromatograms relating to the metabolism studies. This material is available free of charge via the Internet at http://pubs.acs.org.

References

1. Marmor, M. D.; Skaria, K. B.; Yarden, Y. Signal transduction and oncogenesis by ErbB/HER receptors. *Int. J. Radiat. Oncol. Biol. Phys.* **2004,** 58, 903-913.
2. Bazley, L. A.; Gullick, W. J. The epidermal growth factor receptor family. *Endoncr. Relat. Cancer* **2005,** 12, S17-S27.
3. Salomon, D. S.; Brandt, R.; Ciadiello, F.; Normanno, N. Epidermal growth factor receptor-related peptides and their receptors in human malignancies. *Crit. Rev. Oncol. Hematol.* **1995,** 19, 183-232.
4. Normanno, N.; Maiello, M. R.; de Luca, A. Epidermal Growth Factor Receptor Tyrosine kinase inhibitors (EGFR-TKIs): simple drugs with a complex mechanism of action? *J. Cell. Physiol.* **2002,** 194, 13-19.
5. Salomon, D. S.; Brandt, R.; Ciadiello, F.; Normanno, N. Epidermal growth factor receptor-related peptides and their receptors in human malignancies. *Crit. Rev. Oncol. Haematol.* **1995,** 19, 183-232.
6. Woodburn, J. R. Epidermal growth factor receptor and its inhinbitors in cancer therapy. *Pharmacol. Ther.* **1999,** 82, 241-250.

7. Ranson, M.; Sliwkowski, M. X. Perspectives of anti-HER monoclonal antibodies. *Oncology* **2002,** 63, 17-24.

8. Yip, Y. L.; Ward, R. L. Anti-ErbB-2 monoclonal antibodies and ErbB-2 directed vaccines. *Cancer Immunol. Immunother.* **2002,** 50, 569-587.

9. Barker, A. J.; Gibson, K. H.; Grundy, W.; Godfrey, A. A.; Barlow, J. J.; Healy, M. P.; Woodburn, J. R.; Ashton, S. E.; Curry, B. J.; Scarlett, L.; Henthorn, L.; Richards, L. Studies leading to the identification of ZD1839 (IressaTM): an orally active, selective Epidermal Growth Factor Receptor Tyrosine Kinase inhibitor targeted to the treatment of cancer. *Bioorg. Med. Chem. Lett.* **2001,** 11, 1911-1914.

10. Hidalgo, M.; Siu, L. L.; Nemunaitis, J.; Rizzo, J.; Hammond, L. A.; Takimoto, C.; Eckhardt, S. G.; Tolcher, A.; Britten, C. D.; Denis, L.; Ferrante, K.; Von Hoff, D. D.; Silberman, S.; Rowinsky, E. K. Phase I and pharmacologic study of OSI-774, an Epidermal Growth Factor Receptor Tyrosine Kinase inhibitor, in patients with advanced solid malignancies. *J. Clin. Oncol.* **2001,** 19, 3267-3279.

11. Rabindran, S. K.; Discafani, C. M.; Rosfjord, E. C.; Baxter, M.; Floyd, M. B.; Golas, J.; Hallett, W. A.; Johnson, B. D.; Nilakantan, R.; Overbeek, E.; Reich, M. F.; Shen, R.; Shi, X.; Tsou, H.-R.; Wang, Y.-F.; Wissner, A. Antitumor activity of HKI-272, an orally active, irreversible inhibitor of the HER-2 tyrosine kinase. *Cancer Res.* **2004,** 64, 3958-3965.

12. Laheru, D.; Croghan, G.; Bukowski, R.; Rudek, M.; Messersmith, W.; Erlichman, C.; Pelley, R.; Jimeno, A.; Donehower, R.; Boni, J.; Abbas, R.; Martins, P.; Zacharchuk, C.; Hidalgo, M. A phase I study of EKB-569 in combination with capecitabine in patients with advanced colorectal cancer. *Clin. Cancer Res.* **2008,** 14, 5602-5609.

13. Bikker, J. A.; Brooijmans, N.; Wissner, A.; Mansour, T. S. Kinase domain mutations in cancer: implications for small molecule drug design strategies. *J. Med. Chem.* **2009,** 52, 1493-1509.

14. Mishani, E.; Abourbeh, G.; Eiblmaier, M.; Anderson, C. J. Imaging of EGFR and EGFR Tyrosine Kinase overexpression in tumors by nuclear medicine modalities. *Curr. Pharm. Des.* **2008,** 14, 2983-2998.

15. Ping Li, W.; Meyer, L. A.; Capretto, D. A.; Sherman, C. D.; Anderson, C. J. Receptor binding, biodistribution and metabolism studies of ^{64}Cu-DOTA-cetuximab, a PET imaging agent for epidermal growth factor receptor positive tumors. *Cancer Biother. Radiopharm.* **2008,** 23, 158-171.

16. Eiblmaier, M.; Meyer, L. A.; Watson, M. A.; Fracasso, P. M.; Pike, L. J.; Anderson, C. J. Correlating EGFR expression with receptor-binding properties and internalization of ^{64}Cu-DOTA-Cetuximab in 5 cervical cancer cell lines. *J. Nucl. Med.* **2008,** 49, 1472-1479.

17. Mulholland, G. K.; Zheng, Q.-H.; Winkle, W. L.; Carlson, K. A. Synthesis and biodistribution of new C-11 and F-18 labeled epidermal growth factor receptor ligands. . *J. Nucl. Med.* **1997,** 38, P141.

18. Seimbille, Y.; Phelps, M. E.; Czernin, J.; Silverman, D. H. S. Fluorine-18 labeling of 6,7-disubstituted anilinoquinazoline derivatives for positron emission tomography (PET) imaging of tyrosine kinase receptors: synthesis of 18F-Iressa and related molecular probes. *J. Label. Compd. Radiopharm.* **2005,** 48, 829–843.

19. Bonasera, T. A.; Ortu, G.; Rozen, Y.; Krais, R.; Freedman, N. M. T.; Chisin, R.; Gazit, A.; Levitzki, A.; Mishani, E. Potential ^{18}F-labeled biomarkers for epidermal growth factor receptor tyrosine kinase. *Nucl.Med.Biol.* **2001,** 28, 359-374.

20. Yun, C.-H.; Mengwasser, K. E.; Toms, A. V.; Woo, M. S.; Greulich, H.; Wong, K.-K.; Meyerson, M.; Eck, M. J. The T790M mutation in EGFR kinase causes drug resistance by increasing the affinity for ATP. *Proc. Natl. Acad. Sci. U.S.A.* **2008,** 105 2070-2075.

21. Ortu, G.; Ben-David, I.; Rozen, Y.; Freedman, N. M. T.; Chisin, R.; Levitzki, A.; Mishani, E. Labeled EGFR-TK irreversible inhibitor (ML03): *in vitro* and *in vivo* properties, potential as PET biomarker for cancer and feasibility as anticancer drug. *Int. J. Cancer.* **2002,** 101, 360-370.

22. Mishani, E.; Abourbeh, G.; Rozen, Y.; Jacobson, O.; Laky, D.; Ben David, I.; Levitzki, A.; Shaul, M. Novel carbon-11 labeled 4-dimethylamino-but-2-enoic acid [4-(phenylamino)-quinazoline-6-yl]-amides: potential PET bioprobes for molecular imaging of EGFR-positive tumors. *Nucl. Med. Biol.* **2004,** 31, 469-476.

23. Abourbeh, G.; Dissoki, S.; Jacobson, O.; Litchi, A.; Daniel, R. B.; Laki, D.; Levitzki, A.; Mishani, E. Evaluation of radiolabeled ML04, a putative irreversible inhibitor of epidermal growth factor receptor, as a bioprobe for PET imaging of EGFR-overexpressing tumors *Nucl. Med. Biol.* **2007,** 34 55–70.

24. Dissoki, S.; Aviv, Y.; Laky, D.; Abourbeh, G.; Levitzki, A.; Mishani, E. The effect of the [18F]-PEG group on tracer qualification of [4-(phenylamino)-quinazoline-6-YL]-amide moiety—An EGFR putative irreversible inhibitor. *Appl. Radiat. Isot.* **2007,** 65, 1140–1151.

25. Dissoki, S.; Eshet, R.; Billauer, H.; Mishani, E. Modified PEG-anilinoquinazoline derivatives as potential EGFR PET agents. *J. Label. Compd. Radiopharm.* **2009,** 52, 41-52.

26. Kobus, D.; Giesen, Y.; Ullrich, R.; Backes, H.; Neumaier, B. A fully automated two-step synthesis of an ^{18}F-labelled tyrosine kinase inhibitor for EGFR kinase activity imaging in tumors. *Appl. Radiat. Isot.* **2009,** 67, 1977-1984.

27. Torrance, C. J.; Jackson, P. E.; Montgomery, E.; Kinzler, K. W.; Vogelstein, B.; Wissner, A.; Nunes, M.; Frost, P.; Discafani, C. M. Combinatorial chemoprevention of intestinal neoplasia. *Nature Med.* **2000,** 6, 1024 - 1028.

28. Wissner, A.; Overbeek, E.; Reich, M. F.; Floyd, M. B.; Johnson, B. D.; Mamuya, N.; Rosfjord, E. C.; Discafani, C.; Davis, R.; Shi, X.; Rabindran, S. K.; Gruber, B. C.; Ye, F.; Hallett, W. A.; Nilakantan, R.; Shen, R.; Wang, Y.-F.; Greenberger, L. M.; Tsou, H.-R. Synthesis and structure-activity relationships of 6,7-disubstituted 4-anilinoquinoline-3-carbonitriles. The design of an orally active, irreversible inhibitor of the tyrosine kinase activity of the Epidermal Growth Factor Receptor (EGFR) and the Human Epidermal Growth Factor Receptor-2 (HER-2). *J. Med. Chem.* **2003,** 46, 49-63.

29. Samén, E.; Thorell, J.-O.; Fredriksson, A.; Stone-Elander, S. The tyrosine kinase inhibitor PD153035: implication of labeling position on radiometabolites formed in vitro *Nucl. Med. Biol.* **2006,** 33, 1005-1011.

30. Smith, D. A.; Jones, B. C.; Walker, D. K. Design of drugs involving the concepts and theories of drug metabolism and pharmacokinetics. *Med. Res. Rev.* **1996,** 16, 243-266.

31. Tsou, H.-R.; Overbeek-Klumpers, E. G.; Hallett, W. A.; Reich, M. F.; Floyd, M. B.; Johnson, B. D.; Michalak, R. S.; Nilakantan, R.; Discafani, C.; Golas, J.; Rabindran, S. K.; Shen, R.; Shi, X.; Wang, Y.-F.; Upeslacis, J.; Wissner, A. Optimization of 6,7-disubstituted-4-(arylamino)quinoline-3-carbonitriles as orally active, irreversible inhibitors of Human Epidermal Growth Factor Receptor-2 kinase activity. *J. Med. Chem.* **2005,** 48, 1107-1131.

32. Wei, X.; Taylor, R. J. K. *In situ* alcohol oxidation-Wittig reactions. *Tetrahedron Lett.* **1998** 39 3815-3818.

33. Kolb, H. C.; Finn, M. G.; Sharpless, K. B. Click Chemistry: diverse chemical function from a few good reactions. *Angew. Chem. Int. Ed.* **2001,** 40, 2004 - 2021.

34. Tornoe, C. W.; Christensen, C.; Meldal, M. Peptidotriazoles on solid phase: [1,2,3]-triazoles by regiospecific copper(I)-catalyzed 1,3-dipolar cycloadditions of terminal alkynes to azides. *J. Org. Chem.* **2002,** 67, 3057-3064.

35. Hein, C.; Hein, C. D. Click chemistry, a powerful tool for pharmaceutical sciences. *Pharm. Res.* **2008,** 25, 2216.

36. Feldman, A. K.; Colasson, B.; Fokin, V. V. One-pot synthesis of 1,4-disubstituted 1,2,3-triazoles from *in situ* generated azides. *Org. Lett.* **2004,** 6, 3897-3899.

37. Glaser, M.; Arstad, E. "Click Labeling" with 2-[18F]Fluoroethylazide for Positron Emission Tomography. *Bioconjugate Chem.* **2007,** 18, 989-993.

38. Smith, G.; Glaser, M.; Perumal, M.; Nguyen, Q.-D.; Shan, B.; Årstad, E.; Aboagye, E. O. Design, synthesis, and biological characterization of a caspase 3/7 selective isatin labeled with 2-[^{18}F]fluoroethylazide. *J. Med. Chem.* **2008,** 51, 8057-8067.

39. Glaser, M.; Robins, E. G. "Click labelling" in PET radiochemistry. *J. Label. Compd. Radiopharm.* **2009,** 52, 407-414.

40. Rewcastle, G. W.; Palmer, B. D.; Bridges, A. J.; Showalter, H. D. H.; Sun, L.; Nelson, J.; McMichael, A.; Kraker, A. J.; Fry, D. W.; Denny, W. A. Tyrosine kinase inhibitors. 9. Synthesis and evaluation of fused tricyclic quinazoline analogues as ATP site inhibitors of the tyrosine kinase activity of the Epidermal Growth Factor Receptor. *J. Med. Chem.* **1996,** 39, 918-928.

41. Barnes, D. W. Epidermal growth factor inhibits growth of A431 human epidermoid carcinoma in serum-free cell culture. *J. Cell Biol.* **1982,** 93, 1-4.

42. Lipinski, C. A.; Lombardo, F.; Dominy, B. W.; Feeney, P. J. Experimental and computational approaches to estimate solubility and permeability in drug discovery and development settings. *Adv. Drug. Deliv. Rev.* **1997,** 23, 3-25.

43. Abourbeh, G.; Dissoki, S.; Jacobson, O.; Litchi, A.; Daniel, R. B.; Laki, D.; Levitzki, A.; Mishani, E. Evaluation of radiolabeled ML04, a putative irreversible inhibitor of Epidermal Growth Factor Receptor, as a bioprobe for PET imaging of EGFR-overexpressing tumors. *Nucl. Med. Biol.* **2007,** 34 55–70.

44. Wissner, A.; Berger, D. M.; Boschelli, D. H.; Floyd, J., M. Brawner ; Greenberger, L. M.; Gruber, B. C.; Johnson, B. D.; Mamuya, N.; Nilakantan, R.; Reich, M. F.; Shen, R.; Tsou, H.-R.; Upeslacis, E.; Wang, Y. F.; Wu, B.; Ye, F.; Zhang, N. 4-Anilino-6,7-dialkoxyquinoline-3-carbonitrile Inhibitors of Epidermal Growth Factor Receptor Kinase and their bioisosteric relationship to the 4-anilino-6,7-dialkoxyquinazoline Inhibitors. *J. Med. Chem.* **2000,** 43, 3244-3256.

45. Block, D.; Coenen, H. H.; Stöcklin, G. The N.C.A. nucleophilic ^{18}F-fluorination of 1,*N*-disubstituted alkanes as fluoroalkylation agents. *J. Label. Compd. Radiopharm.* **1987,** 24, 1029-1042.

46. Haka, M. S.; Kilbourn, M. R.; Watkins, G. L.; Toorongian, S. A. Aryltrimethylammonium trifluoromethanesulfonates as precursors to aryl [^{18}F]fluorides: Improved synthesis of [^{18}F]GBR-13119. *J. Label. Compd. Radiopharm.* **1989,** 27, 823-833.